Improved models, improved information? Exploring how climate change impacts pollen, influenza, and mold in Berlin and its surroundings

Langendijk, Gaby S.; Rechid, Diana; Jacob, Daniela

Published in:
Urban Climate

DOI:
10.1016/j.uclim.2022.101159

Publication date:
2022

Document Version
Publisher's PDF, also known as Version of record

Urban Climate 43 (2022) 101159

Contents lists available at ScienceDirect

Urban Climate

journal homepage: www.elsevier.com/locate/uclim

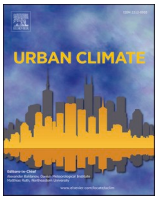

Improved models, improved information? Exploring how climate change impacts pollen, influenza, and mold in Berlin and its surroundings

Gaby S. Langendijk [a,b,*], Diana Rechid [a], Daniela Jacob [a,b]

[a] Climate Service Center Germany (GERICS), Helmholtz-Zentrum Hereon, Fischertwiete 1, 20095 Hamburg, Germany
[b] Faculty of Sustainability, Leuphana University of Lüneburg, Universitätsallee 1, 21335 Lüneburg, Germany

ARTICLE INFO

Keywords:
Climate change impact
Convection-permitting model
Added value
Regional climate model
Pollen
Mold
Influenza
Humidity
Berlin

ABSTRACT

Urban decision makers rely on evidence-based climate information tailored to their needs to adequately adapt and prepare for future climate change impacts. Regional climate models, with grid sizes between 10–50 km, are a useful outset to understand potential future climate change impacts in urban regions. Recently developed convection-permitting climate models have grid sizes smaller than 5 km, and better resolve atmospheric processes related to the land surface like convection, and complex terrain such as cities. This study investigates how the convection-permitting model REMO simulates changes in climate conditions in the urban-rural context, compared to its conventional hydrostatic version. We analyze three impact cases: influenza spread and survival; ragweed pollen dispersion; and indoor mold growth. Simulations are analyzed for the near future (2041–2050) under emission scenario RCP8.5. Taking the Berlin region as a testbed, we show that the change signal (positive or negative impact) reverses for the 3 km compared to the 12.5 km grid resolution for the impact cases pollen, and mold, indicating added value. For influenza, the convection-permitting resolution intensifies the decrease of influenza days under climate change. The results show the potential of convection-permitting simulations to generate improved information about climate change impacts for urban regions to support decision making.

1. Introduction

High-quality, science-based climate information for cities and its surroundings is crucial for urban decision makers and dwellers in order to prepare for and adapt to climate change (Baklanov et al., 2018; Rosenzweig et al., 2018). This information shall be tailored to the needs of urban decision makers, suitable for their specific application and context (Bai et al., 2018; Baklanov et al., 2018). Urban areas have distinct climatological characteristics that differ from its surroundings, e.g. the urban heat and dry island effect (e.g. Langendijk et al., 2019; Lokoshchenko, 2017; Masson et al., 2020). Therefore, climate change may manifest differently in cities than its direct surroundings. Environmental factors, and more specifically meteorological conditions, are key drivers for climate change impacts in urban areas (Masson et al., 2020; Rosenzweig et al., 2018).

Models are a useful outset to understand changes in meteorological conditions in cities as a result of climate change. Regional

* Corresponding author at: Climate Service Center Germany (GERICS), Helmholtz-Zentrum Hereon, Fischertwiete 1, 20095 Hamburg, Germany.
E-mail address: gaby.langendijk@hereon.de (G.S. Langendijk).

https://doi.org/10.1016/j.uclim.2022.101159
Received 21 September 2021; Received in revised form 17 February 2022; Accepted 20 March 2022
Available online 31 March 2022

climate models simulate the Earth's key physical climate processes and their interactions. They divide the Earth's surface and overlying atmosphere into a giant grid. The model calculates meteorological variables, such as temperature, humidity and precipitation, for each grid cell. The horizontal grid size, or "grid resolution", of regional climate models are typically in the range of 50–10 km, with around 20–30 vertical layers (Jacob et al., 2020). Grid sizes up to 20–10 km allow for the simulation of larger urban areas under longer climatological timescales, using simple urban schemes. The models are commonly unable to capture intra-city differences and fine-scale urban climate processes (Langendijk et al., 2019).

The newly developed, so-called, convection-permitting (CP) climate models are high-resolution regional models of the Earth's climate that have a horizontal grid size of less than 5 km, and around 40–50 vertical layers. CP models better resolve the land surface and convective processes, leading to improved representation of small-scale processes in the atmosphere and complex terrain, such as cities (Argüeso et al., 2016; Ban et al., 2021, 2014; Coppola et al., 2020; Kendon et al., 2021; Prein et al., 2015). This can result in clear improvements, so-called added value, to simulate climate change impacts, which subsequently allows for better-informed decision making (Di Luca et al., 2015). There has only been limited research on the added value of CP models to simulate and understand climate change impacts in urban areas compared to its surroundings. Therefore, this research explores the potential of convection-permitting models to improve the simulation of climate change impacts in urban areas and its surroundings. The study compares regional climate model output on the 12.5 km grid resolution and the 3 km convection-permitting resolution, using Berlin and its surroundings as testbed.

1.1. Impact cases

To investigate the effect of the convection-permitting scale on climate conditions related to climate change impacts, three so-called impact cases are defined: influenza spread and survival, ragweed pollen dispersion, and indoor mold growth. These impact cases are selected because they all have direct or in-direct effects on human health, and they have been hardly investigated by previous studies, especially not under future climate change and in the urban-rural context. The three impact cases are defined by meteorological conditions, foremost underpinned by the variables humidity and temperature. The change in meteorological conditions for each impact case under climate change is studied. The following section introduces the impact cases and defines the meteorological conditions that favor the cases based on existing literature. This study particularly considers humidity and temperature. Humidity is expressed as specific humidity (SH), which is the amount of water vapor in relation to the total mass of water vapor and air combined, expressed in kilograms of water vapor per kilogram of moist air (kg/kg). In addition, it considers relative humidity (RH), the saturation of the air compared to the water vapor the fully saturated air could contain at a specific temperature, expressed as a percentage (%).

1.1.1. Influenza survival and transmission

The infectious disease influenza, commonly known as "flu", is one of the most deadly of all airborne and upper-respiratory infections (Fuhrmann, 2010). Much of the observed wintertime increase of mortality in temperate regions is attributed to seasonal influenza (Shaman et al., 2010). On average, 22,000 deaths and over 3 million hospitalizations in USA are attributed to influenza each year (Fuhrmann, 2010). In 2017/18 around 25.100 people died in Germany during the most deadly influenza wave in 30 years (RKI, 2019). A previous study investigating the historic time period 1970–2016 showed long-term climate variations influenced the influenza-like illness incidence rates in the Netherlands, through changes in absolute humidity and temperature (Caini et al., 2018). Although of profound interest, the potential impacts of future climate change on influenza epidemics is poorly understood, and no studies have directly investigated this interplay (Chong et al., 2020; Goodwins et al., 2019).

The connection between humidity and influenza is likely multifactorial, including impacts on virus stability and viability, host susceptibility, and human behavior (Davis et al., 2016). However, many studies show low humidity, often occurring in combination with low temperatures, is the predominant factor defining the transmission and survival of the influenza virus (Davis et al., 2016; Lowen et al., 2007; Lowen and Steel, 2014; Marr et al., 2019; Park et al., 2020; Peci et al., 2019; Shaman et al., 2011). Model predictions suggest that approximately half of the average seasonal differences in US influenza mortality can be explained by seasonal differences in absolute humidity alone (Barreca and Shimshack, 2012). Soebiyanto et al. (2015) show a clear inverse relationship between specific humidity and influenza exists in Europe, and particularly in Berlin. Two hypotheses are proposed by Shaman and Kohn (2009) to explain the humidity-influenza relationship: (i) virus-laden droplet nuclei are more efficiently produced at lower humidity because of increased evaporation of expelled droplet particles, therefore more virus remains longer in the atmosphere; (ii) influenza virus survival increases as humidity decreases, such that the airborne virus remains viable longer at lower humidity levels (Shaman and Kohn, 2009).

Literature indicates a controversy of the appropriate humidity variable selection to study the humidity and influenza relationship. Many studies showed a relationship between low RH and influenza virus transmission and/or survival (Lowen et al., 2007; Lowen and Steel, 2014; Marr et al., 2019; Noti et al., 2013; Park et al., 2020). Though other studies show that SH or absolute humidity (AH) would be preferable over RH to investigate the humidity-influenza relationship, as SH/AH would constrain the transmission and survival of influenza more significantly than RH (Barreca and Shimshack, 2012; Chong et al., 2020; Peci et al., 2019; Shaman et al., 2011; Shaman and Kohn, 2009). Considering this discussion, specific humidity is selected to define the influenza threshold for this research.

A non-linear relationship between influenza transmission and survival exists that is most sensitive to low humidity values, leading to increases in the spread of influenza among humans (Barreca and Shimshack, 2012; Beest et al., 2013; Shaman et al., 2011, 2010). Specific humidity levels below approximately 6 g of water vapor per kilogram of air (0.006 kg/kg) are associated with increases in influenza mortality (Barreca and Shimshack, 2012). This is also in line with studies by Shaman et al., (2011, 2010 especially Fig. 1). Cold temperatures around ~5 °C optimize the influenza conditions (Lowen and Steel, 2014; Park et al., 2020). The Robert Koch

Table 1
Defined humidity thresholds and meteorological conditions per impact case: influenza spread and survival; ragweed pollen dispersion; and in-door mold growth.

	Influenza	Pollen	Mold
Meteorological variables	SH < 0.006 kg/kg & 2–6 °C	RH < 60%	RH > 80% & 10 °C–40 °C
Months	December – March	July – October	entire year
Time/days	–	5 am until 2 pm	2–10 consecutive days

Institute (RKI, 2020) points out that influenza is mainly occurring in winter months in Brandenburg and Berlin. This is confirmed by Soebiyanto et al. (2015) who indicate influenza is mainly prevalent in December – March in Berlin.

The selected meteorological threshold to investigate the influenza impact case is therefore, SH < 0.006 kg/kg, jointly with low temperatures from 2 °C up to 6 °C, for the period December – March (Table 1).

1.1.2. Ragweed pollen dispersion

Ragweed (*Ambrosia artemisiifolia* L.) is an invasive annual weed, native from North America, and currently one of the main allergenic species in Europe (Cunze et al., 2013; Ghiani et al., 2016). Ragweed is expected to particularly expand its range due to climate change in Northern Europe (Cunze et al., 2013; Storkey et al., 2014). In this regard, Hamaoui-Laguel et al. (2015) estimate that by 2050 airborne ragweed pollen concentrations will be about four times higher than they are now in Europe. Climate change could increase the length and severity of the pollen season and, as a consequence, the related pollen allergy (D'Amato and Cecchi, 2008; Ziska et al., 2003).

Due to regional urbanization-induced temperature and higher CO2 levels in cities ragweed grows faster, flowers earlier, and produces significantly greater ragweed pollen in urban than rural areas (Bergmann et al., 2012; Ziska et al., 2003). Epidemiological studies have demonstrated that urbanization, high levels of vehicle emissions and western lifestyles are correlated to an increase in the frequency of pollen-induced respiratory allergy, prevalent in people who live in urban areas compared to rural areas (D'Amato and Cecchi, 2008). Reinhardt et al. (2003) estimated the consequential costs for the treatment of patients allergic to ragweed to lie between €19 and €50 million per year for Germany under current climate conditions. In Berlin and its surroundings, extensive ragweed populations are reported and ragweed pollen are measured (Buters et al., 2015; Kannabei et al., 2013; Zink et al., 2012). Around 15– 18% of Berlin's population suffers from a pollen allergy, resulting in approximately 500,000 –615,000 affected people just in this city (Bergmann et al., 2012).

Different meteorological and human factors influence pollen growth, length of the season, or transport through the atmosphere (e.g. Sofiev et al., 2013). There is specific evidence that low relative humidity, often occurring with higher temperatures, favors the release of pollen locally, directly enhancing pollen dispersion rates, while high humidity is associated with lower airborne pollen concentrations (Bianchi et al., 1959; D'Amato and Cecchi, 2008; Silverberg et al., 2015; Sofiev et al., 2013; Zink et al., 2012). Zink et al. (2012) found that the majority of the pollen in Germany originated in local areas. The ragweed pollen release period from a single flower lasts only up to 6 h (Prank et al., 2013). The pollen release can be strongly reduced, or even halted, by high relative humidity associated with rain, which can cover wider areas than the rain event itself (Sofiev et al., 2013).

Ragweed pollen emissions are considered a threshold process, dominated by low relative humidity, with a threshold of around <60% RH (Bianchi et al., 1959; Menut et al., 2014; Sofiev et al., 2013; Zink et al., 2012). The main ragweed flowering season is from August to September in Europe, however flowers can be found from July to October in the Berlin region (Kannabei et al., 2013; Liu et al., 2016; Prank et al., 2013). The end of flowering has been found to be correlated spatially and temporally with the onset of the first frost (Kannabei et al., 2013; Storkey et al., 2014). Local ragweed pollen emission mainly takes place during the morning hours: it starts shortly after sunrise and continues until early afternoon (Bianchi et al., 1959; Dingle et al., 1959; Laaidi and Laaidi, 1999; Zink et al., 2012).

The selected humidity threshold for the pollen impact case is RH < 60%, from 5 am until 2 pm, during July – October (Table 1).

1.1.3. Indoor mold growth

Indoor mold is a fungal growth that develops on building materials, expedited by particular outdoor temperatures, and humidity conditions (Sedlbauer, 2001). In Germany mold is one of the main causes of damage to buildings. The "Third Report on Building Damages" by the Federal Government of Germany estimated the costs resulting from mold fungi damages to amount more than 200 million Euro per year (Bundesministerium für Raumordnung, 1995). In addition, extensive mold growth in buildings can negatively affect human health, by causing and enhancing respiratory complications and related diseases such as asthma (Davis et al., 2016). Studies show that historic buildings are particularly prone to mold growth and damage (Curtis, 2010; Hao et al., 2020; Huijbregts et al., 2012). In Berlin every fourth house is built in the 1920s/30s, and around 50% of the building are older than 1960 (SSW, 2018).

A literature review by Hao et al. (2020) indicates that moisture risks are more likely to occur in buildings due to changes in the external climate and subsequent changes in the indoor climate. Leissner et al. (2015) particularly project higher mold risks in Northern parts of Germany by the mid as well as by the end of the century, based on derived mold index from regional climate model projections. A study by Huijbregts et al. (2012) found mold growth will increase due to climate change for two historic museum buildings in the Netherlands and Belgium, particularly driven by rising relative humidity levels.

The growth and spreading of mold fungi mainly depends on the climatic boundary conditions at the surfaces of construction parts and inside buildings. The decisive parameters are relative humidity, temperature and the corresponding substrate (Huijbregts et al.,

2012; Johansson et al., 2012; Leissner et al., 2015; Lourenço et al., 2006; Ojanen et al., 2010; Pietrzyk, 2015; Sedlbauer, 2001; Viitanen and Ojanen, 2007; Viitanen et al., 2010). Despite the complexity of indoor climate, a direct correlation between internal and external conditions has been found and verified (Hao et al., 2020), including a strong correlation between indoor and outdoor absolute humidity (Nguyen et al., 2014). Outside relative humidity, in combination with temperature, is of critical importance to indoor mold growth.

Many studies identify conditions around >80% relative humidity and temperatures of 10 °C–40 °C to be favorable for mold growth (Johansson et al., 2012; Leissner et al., 2015; Ojanen et al., 2010; Sedlbauer, 2001; Viitanen et al., 2010). Sedlbauer (2001 (especially Figure 9)) shows 2– 16 consecutive days of favorable mold growth conditions enhance mold expansion.

The selected meteorological condition for the mold impact case is RH >80% and 10 °C– 40 °C, during the entire year. 2–10 consecutive days of favorable mold growth conditions are also considered.

2. Methods

2.1. Study area

Berlin and its surroundings is selected as the case-study region. The capital of Germany, Berlin, is a large-scale city with around 3.6 million inhabitants covering approximately 891.1 km^2 (Amt für Statistik Berlin-Brandenburg, 2020), located in-land at approximately

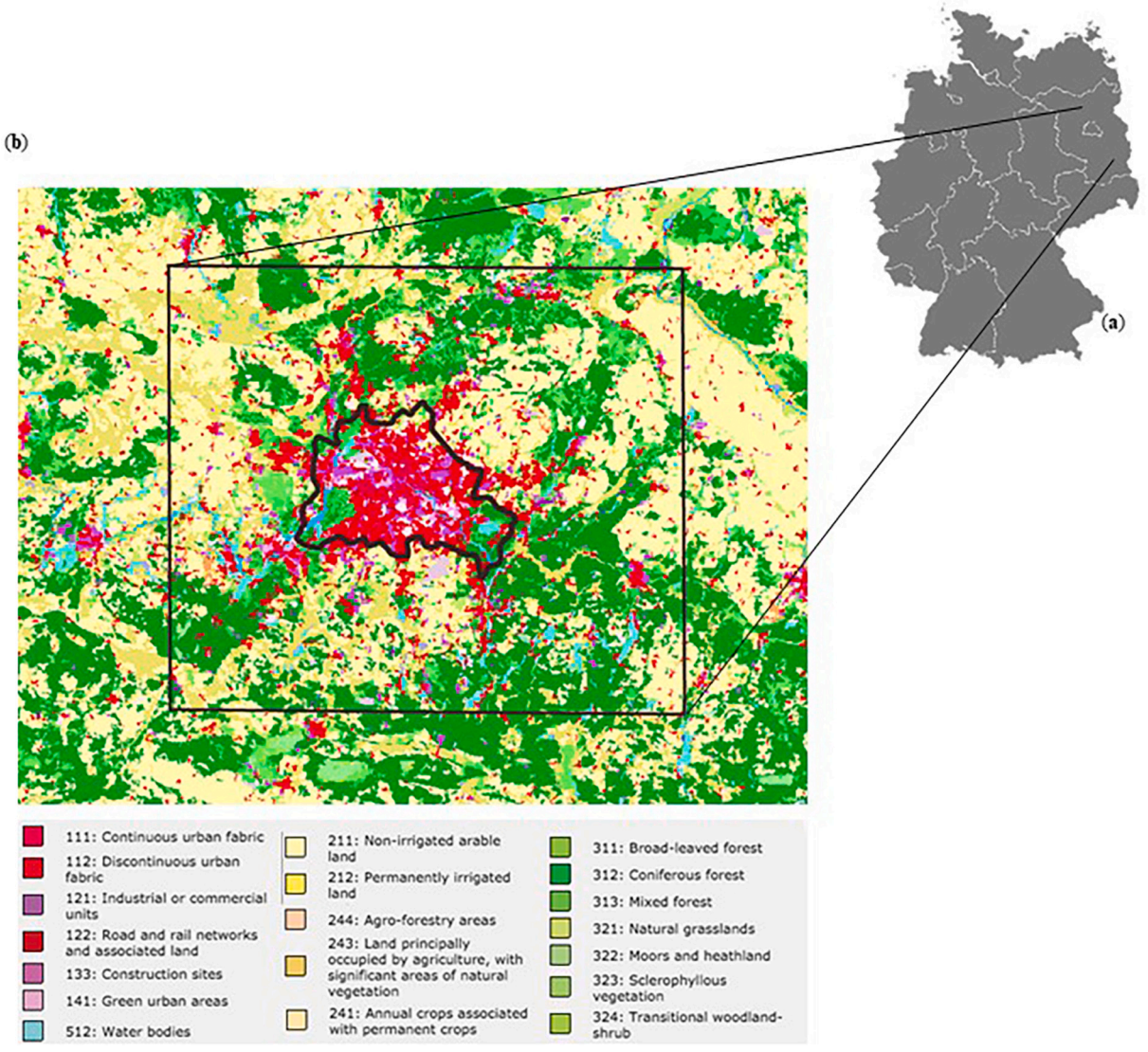

Fig. 1. Research area. (**a**) Germany and (**b**) a land-cover map indicating Berlin's administrative boundaries (black polygon) and research domain including the surroundings (black rectangular). Land cover following CORINE land cover map (EEA, 2000; Langendijk et al., 2019).

52.52° N, 13.4° E. The land cover of Berlin's surroundings is roughly 50% agricultural and grass land, 36% forest and 14% build up areas and water bodies (Fig. 1b) (Amt für Statistik Berlin-Brandenburg, 2020). Berlin and its surroundings are particularly suitable to investigate urban-rural contrasts using regional climate model output data, because of the relatively flat regional topography, Berlin's large city size, and the distinct urban-rural landscape heterogeneity. The primary investigated domain is approximately 140 km by 140 km centered around Berlin (black rectangular, Fig. 1b).

2.2. Models, data, and analyses

To evaluate the performance of the regional climate model used to investigate the Berlin region, observations are compared with model output data driven by the ERA-Interim reanalysis dataset on 12.5 km (0.11°) and 3 km (0.0275°) spatial resolution, by respectively the regional climate model REMO, and its non-hydrostatic convection-permitting version (REMO-NH) (Ban et al., 2021; Lowe et al., 2020). REMO is a three dimensional, hydrostatic limited-area model (Jacob et al., 2012; Kotlarski et al., 2014), originating from the 'Europa-Modell' of the German Weather Service (DWD) (Majewski, 1991). The physical parameterizations are largely based on the global climate model ECHAM-4 (Roeckner et al., 1996) and have been further developed over the course of the last decades. Model specifications can be found in Jacob et al. (2012) and in Jacob and Podzun (1997). The non-hydrostatic convection-permitting model version, REMO-NH, directly resolves the vertical momentum equation, leading to a better representation of small-scale mesoscale circulations and convection (Goettel, 2009; Langendijk et al., 2021).

For the model evaluation, relative humidity, specific humidity and 2-m temperature are investigated at a daily time-step, averaged over each year during the ERA-interim driven period 2000–2009. The REMO output data used for this study was produced as part of the European Climate Prediction (EUCP) project (Ban et al., 2021; Lowe et al., 2020). In-situ station observations are obtained from the DWD data store (DWD, 2021), for five stations in Berlin and five in the surroundings. The locations of the observational stations are presented in the appendices, Fig. A1. The DWD does not provide in-situ observations for specific humidity. Therefore specific humidity is derived from observed mean daily vapor pressure (e) in hPa and air pressure (P) in hPa from DWD in-situ station observations (DWD, 2021), using the following formula (Stull, 2017):

$$Specific\ humidity = \frac{\varepsilon^* e}{P - e^*(1-\varepsilon)} \tag{1}$$

Where $\varepsilon = 0.622$ g vapor/g dry air is the ratio of gas constants for dry air to that for water vapor.

The land cover scheme of REMO follows a tile approach, based on three basic land surface types; land, water, and sea ice. Subgrid fractions are specifying further land cover types, including an urban sub-fraction. These fractions are not assumed to be located in a specific area of a grid box, but cover a percentage of the total grid box area, together summing up to 100% (Rechid and Jacob, 2006; Semmler, 2002). The urban fraction per grid box for the Berlin region is presented in Fig. 2. For the urban sub-fraction, the REMO model follows the so-called 'bulk' approach. Sealed urban areas are represented as a rock surface, which is described in the model by a relatively high roughness length, high albedo, and no water storage capacities (Langendijk et al., 2019). Langendijk et al. (2019) indicate that the simple urban bulk-scheme shows the urban rural contrast for temperature and humidity variables under climate change. The simple scheme is less skilled in simulating the timing of the peak of the urban heat island at night.

A consistent masking approach is developed (following Langendijk et al., 2021) to define the urban area in the 12.5 km and 3 km model output data to allow for coherent analysis across grid resolutions. The urban area contains all the grid cells with an urban fraction larger than 0.3 as prescribed by the REMO land surface cover scheme within the administrative boundaries of Berlin (Black polygon, Fig. 1b). The masks for the surroundings include all grid boxes outside the city mask and within the primary domain of interest of approximately 140 km by 140 km centered around Berlin (black rectangular, Fig. 1b). This approach is followed for both horizontal resolutions. The resulting city masks for the 12.5 km and 3 km grid resolutions cover relatively similar areas for Berlin, with the 3 km mask capturing the actual city extent and boundaries more accurately (Appendices: Fig. A3).

To give insight into the model performance compared to observations, the following statistical measures are calculated for the averaged annual mean for the ERA-interim driven period (2000– 2009) for Berlin and its surroundings, as well as for the averaged

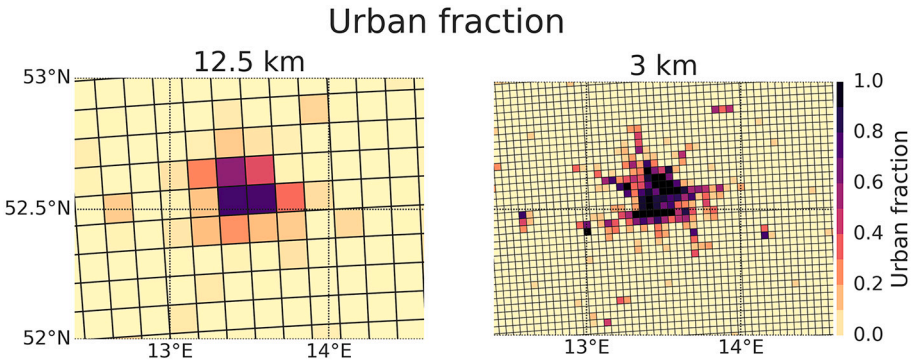

Fig. 2. The urban fraction per grid box of the REMO land surface scheme, for the 12.5 km and 3 km grid resolutions.

monthly data, respectively called the annual cycle, for the ERA-interim driven period (2000– 2009) for Berlin:

- *Root mean square error (RMSE):* absolute measure of the overall error in the estimates relative to the observed values, expressed in the same units and scale as the data itself. It can take any positive value with zero indicating a perfect lack of error.
- *Mean bias error (MBE):* measures the extent to which the estimated value deviates from the observed value. It can take any value, with negative values indicating systematic under-estimation and positive values, over-estimation, and zero indicating a perfect lack of bias.
- *Pearson correlation coefficient:* varies between -1 and $+1$ with 0 implying no correlation. Correlations of -1 or $+1$ imply an exact linear relationship.
- *Standard Deviation (St. Dev.):* a measure of the amount of variation or dispersion of a set of values. A low standard deviation indicates that the values tend to be close to the mean of the set, while a high standard deviation indicates that the values are spread out over a wider range.

Table 2
Statistical outcomes for the annual cycle, RMSE, MBE and Pearson correlation coefficient for relative humidity, specific humidity, and temperature, comparing monthly mean observations with the 12.5 km and 3 km grid resolution, for Berlin, for the ERA-interim period (2000–2009). The green marking shows where the 3 km outperforms the 12.5 km grid resolution, compared to observations.

Relative Humidity	**Jan.**	**Feb.**	**March**	**April**	**May**	**June**	**July**	**Aug.**	**Sept.**	**Oct.**	**Nov.**	**Dec.**
12.5 km												
RMSE (%):	7.53	8.57	6.56	6.20	4.29	3.73	4.84	3.66	3.29	5.09	4.60	5.87
MBE (%):	-7.14	-8.12	-6.04	-4.32	-2.62	-2.22	-2.62	-1.47	0.69	4.23	2.92	-4.32
Pearson corr.:	0.43	0.45	0.83	0.47	0.47	0.36	-0.12	0.34	0.44	0.31	0.48	0.05
3 km												
RMSE (%):	10.73	13.45	15.44	17.40	8.96	4.46	4.39	3.01	3.34	4.33	3.62	8.87
MBE (%):	-10.43	-13.24	-15.10	-17.07	-7.79	-3.14	-2.87	-0.48	1.39	2.73	-2.18	-8.16
Pearson corr.:	0.13	0.33	0.69	0.66	0.09	0.33	0.08	0.33	0.52	0.16	0.51	0.02
Specific Humidity ***12.5 km***												
RMSE (kg/kg):	0.0003	0.0003	0.0006	0.0008	0.0008	0.0011	0.0013	0.0010	0.0008	0.0003	0.00032	0.0003
	-	-	-	-	-	-		-	-	-		-
MBE (kg/kg):	0.0002	0.0003	0.0005	0.0007	0.0007	0.00095	-0.0012	0.00094	0.0007	0.0001	0.00020	0.0001
Pearson corr.:	0.74	0.81	0.61	0.93	0.85	0.51	0.66	0.78	0.85	0.91	0.72	0.83
3 km												
RMSE (kg/kg):	0.0005	0.0005	0.0008	0.0012	0.0011	0.0010	0.0010	0.0012	0.0007	0.0004	0.00027	0.0005
	-	-	-	-	-	-		-	-	-	-	-
MBE (kg/kg):	0.0004	0.0005	0.0007	0.0011	0.0010	0.00087	-0.0009	0.00089	0.0006	0.0002	0.00016	0.0004
Pearson corr.:	0.79	0.84	0.61	0.93	0.86	0.61	0.61	-0.36	0.86	0.90	0.77	0.89
2-m Temperature ***12.5 km***												
RMSE (°C):	1.05	0.94	1.11	0.71	0.95	1.20	1.07	0.93	1.11	0.87	0.96	1.08
MBE (°C):	0.63	0.79	0.43	-0.17	-0.47	-0.91	-0.86	-0.68	-0.92	-0.49	0.63	0.73
Pearson corr.:	0.68	0.85	0.87	0.96	0.77	0.57	0.76	0.89	0.90	0.89	0.86	0.88
3 km												
RMSE (°C):	0.77	0.93	1.49	1.63	1.14	0.96	0.69	0.66	1.12	0.81	0.88	0.61
MBE (°C):	0.20	0.80	1.11	1.46	0.47	-0.44	-0.21	-0.44	-0.82	-0.21	0.66	0.40
Pearson corr.:	0.77	0.87	0.85	0.96	0.69	0.69	0.73	0.91	0.85	0.89	0.89	0.96

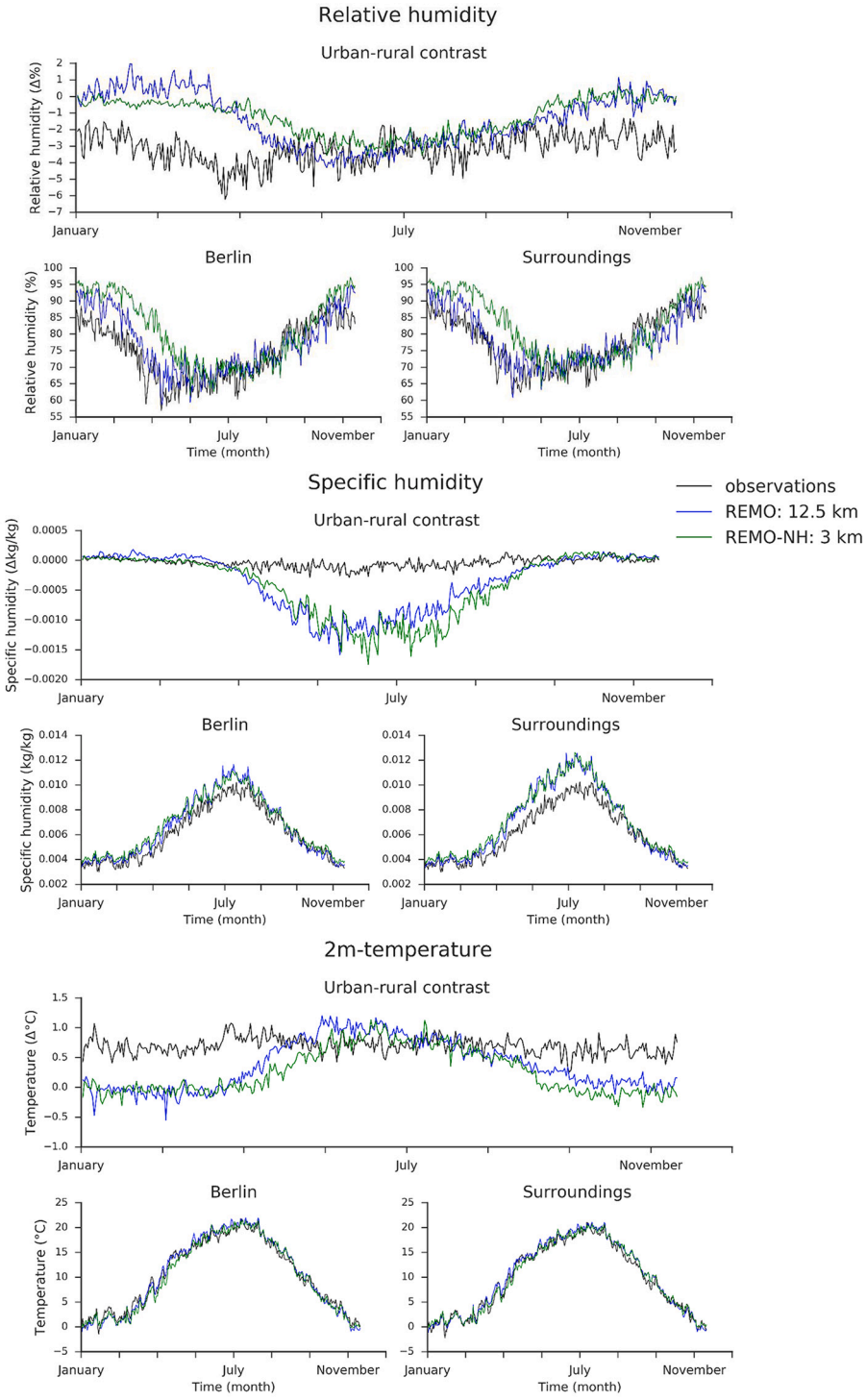

Fig. 3. Annual cycle for daily observations (black), 12.5 km grid resolution (blue) and 3 km grid resolution (green), for relative humidity, specific humidity and 2-m temperature, 10-year mean for the ERA-interim period (2000– 2009). The urban-rural difference is calculated by subtracting the results for the surroundings from those for Berlin. (For interpretation of the references to colour in this figure legend, the reader is referred to the web version of this article.)

In order to conduct the calculations, the model output data is spatially averaged over the grid boxes representing Berlin (black polygon Fig. 1, Appendices: Fig. A3) and its surroundings (black rectangle Fig. 1). The observations are averaged over the different stations, respectively for Berlin and its surroundings (Appendices: Fig. A2). The median, and range of the station measurements are relatively similar, except for Berlin-Alexanderplatz (Appendices: Fig. A2). This station data is slightly warmer and less moist (RH) compared to other stations in Berlin. Probably because the station is located in the city center surrounded by a sealed surface (Appendices: Fig. A1).

The analysis of the impact cases, influenza, pollen, and mold, aims to understand the added value on the 3 km grid resolution, compared to the 12.5 km grid resolution, to simulate climate change impacts in the Berlin region. The REMO model output data for the 12.5 km and the 3 km (REMO-NH) grid resolutions are utilized for the historical time period (1996–2005) and a near-term future time period (2041–2050) under the emission scenario RCP8.5 (Moss et al., 2010), forced by the global climate model MPI-ESM-LR (Stevens et al., 2013). The REMO output data was produced as part of the European Climate Prediction (EUCP) project (Ban et al., 2021; Lowe et al., 2020).

Using the above-mentioned REMO model data, the specified meteorological conditions for each impact case are investigated (Table 1). Firstly, the change in the occurrence of the days that fulfill the respective conditions is calculated. The number of days on which the impact case occurs within each decade is then divided by ten years, resulting in the mean projected change of days/year (d/yr) for each respective time period (historical and future). Secondly, consecutive periods of days under or above the thresholds are calculated for each impact case, following the same rational. The change in d/yr between the future decade and the historical decade is referred to as "change signal" in this research. To calculate a robust climate change signal, averaging over a time period of 20– 30 years in the future as well as over a 20 –30 years historical time period would be required (Hawkins et al., 2020; IPCC, 2013). Due to limited computing power convection-permitting simulations are currently only available for decades. Therefore, this study shows the "change signal", which provides an indication of the climate change signal as it carries the fingerprint of climate change. The following comparisons are examined throughout the analysis: the 12.5 km grid resolution vs. the 3 km grid resolution; the historical time period (1996 2005) vs. the near-term future time period (2041– 2050); and Berlin vs. its surroundings. The near-term future period (2041–2050) is particularly relevant for policy timeframes, as (urban) decision makers tend to be specifically interested in timespans ranging from multi-annual up to the near-term future (Lauwaet et al., 2017).

3. Results

3.1. Model performance across grid resolutions

The outcomes of the model evaluation show that the REMO model, on both the 12.5 km and 3 km grid resolution performs reasonably in line with the observations for Berlin and its surroundings, based on the statistical tests (Table 2, Appendices: Table A1). For the annual mean values averaged over the period 2000–2009, the 12.5 km grid resolution is frequently outperforming the 3 km convection-permitting resolution, particularly for specific and relative humidity. For temperature, the surroundings show an improvement for the RMSE and MBE on the 3 km resolution compared to the 12.5 km resolution. Worth noting, the RH urban-rural contrast shows a slight improvement for the RMSE and the Pearson correlation coefficient (Appendices: Table A1).

The statistical values for the annual cycle show more improvements than the annual mean values for the 3 km grid resolution, in Berlin. The REMO model outputs for relative humidity shows better correspondence with observations on the 3 km resolution than the 12.5 km resolution for the months August, October, and November (RMSE and MBE), but the model is performing worse during the period from January to April (Table 2). This implies potential improved capability of REMO-NH to simulate the pollen impact case, as the relative humidity threshold occurs in July – October. The 3 km resolution shows improvements for specific humidity in Berlin during the summer months June – August, and in November (RMSE and MBE) (Table 2). The Pearson correlation coefficient is higher for 8 out of 12 months for the 3 km resolution compared to the 12.5 km resolution. This improvement, particularly for the months December – March, increases the confidence that the 3 km resolution may improve the simulations for the influenza impact case. For temperature, the 3 km resolution shows improvements in Berlin for almost all months, except March, April and May (RMSE, and/or MBE, and/or Pearson) (Table 2). This may lead to improved simulation of the impact cases that co-depend on temperature, respectively influenza and mold.

These results are underpinned by Fig. 3, showing the time series of the mean annual cycle, averaged over 2000–2009, for Berlin and its surroundings. For relative humidity the REMO model results are in line with the observations for the summer months up to October. The model simulations overestimate relative humidity values for winter and spring, in Berlin and its surroundings. The relative humidity urban-rural contrast shows a similar pattern, and is underestimated in the winter. The 3 km resolution shows an improvement compared to the 12.5 km grid resolution, mainly in January to March. For specific humidity, the models overestimate SH in summer, which is larger for the surroundings than Berlin. This leads to an overestimation of the specific humidity urban-rural contrast in summer months. The REMO model results are largely in line with observations for temperature, for Berlin and its surroundings. The temperature urban-rural contrast, is underestimated in winter months. This can explain the underestimation of the RH urban-rural contrast in the same months, because temperature and RH are closely related. The temperature urban-rural contrast underestimation in winter is most probably caused by the absence of anthropogenic heat in the REMO model, and the limited capacity of the bulk scheme to retain warmth (Jin et al., 2021).

A clear urban-rural difference between Berlin and its surroundings is detectable on the spatial maps presenting the mean for the period 2000–2009, in Fig. 4. Berlin is less humid (SH: ~0.0011 kg/kg, RH: ~2%) and warmer (~0.5 °C) than its surroundings for both spatial resolutions. The 3 km grid resolution is overall more moist (RH and SH) in the Berlin region. There is more detail visible on the 3 km than the 12 km spatial resolution. For instance, the city boundaries of Berlin and the suburbs (urban-rural transition) become

visible on the 3 km resolution, as well as a decrease in temperature and an increase in humidity can be detected around the river Spree (Fig. 4). This enhanced level of detail on the 3 km resolution can be mainly explained by the increase of the amount of grid boxes with urban fractions and better resolving the land surface on the 3 km grid resolution (Fig. 2).

In summary, the model evaluation shows that the REMO model, on the 12.5 km and 3 km grid resolution, is performing reasonably in line with the observations. Statistical improvements are found on the 3 km resolution for specific months for the different variables, potentially indicating that the 3 km resolution may better simulate the variables that underpin the meteorological conditions for the impact cases. Enhanced spatial detail is clearly detectable on the 3 km compared to the 12.5 km grid resolution.

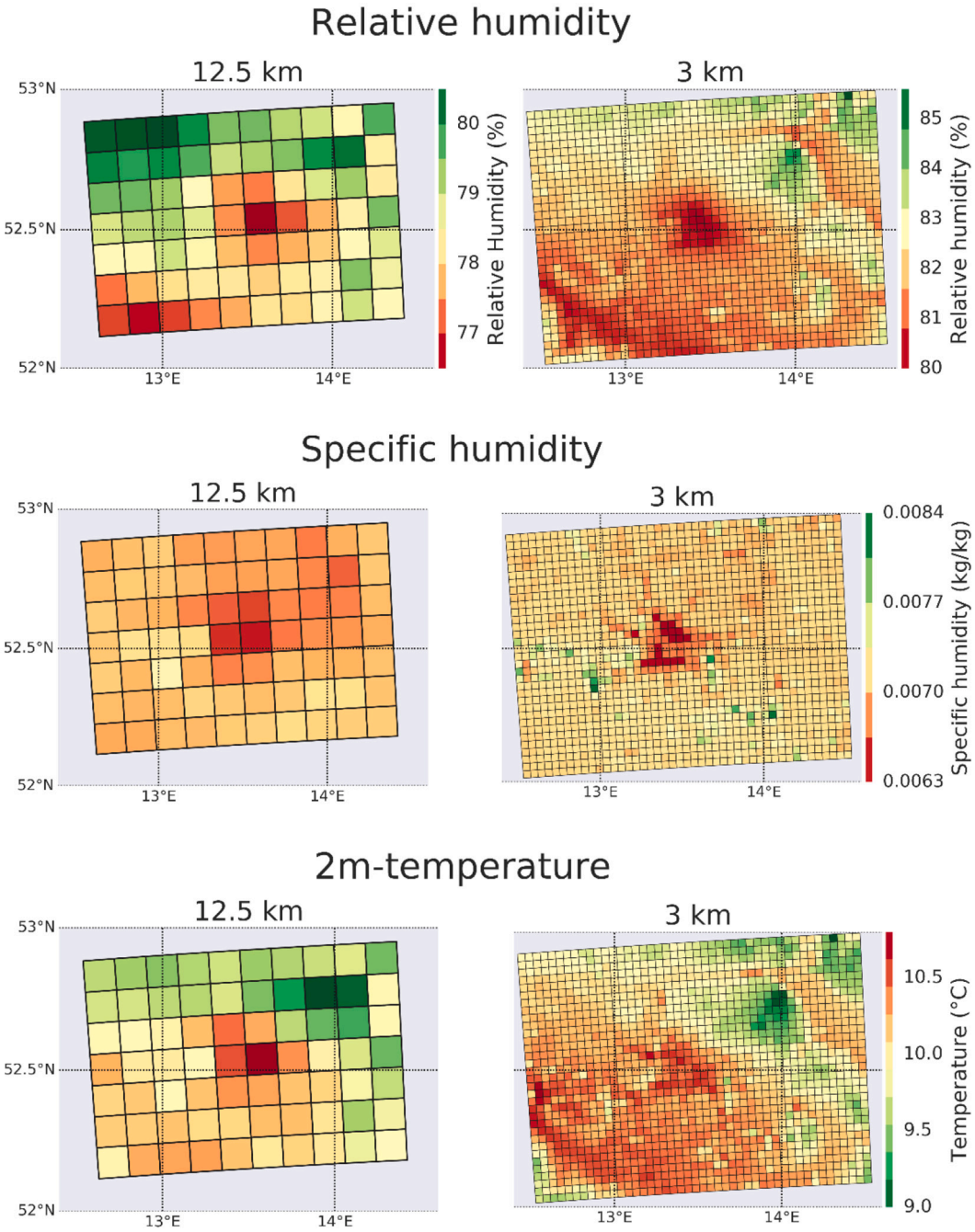

Fig. 4. Spatial maps for the Berlin region on the 12.5 km (left) and 3 km (right) grid resolution, showing the 10-year mean (2000–2009) for relative humidity, specific humidity and 2 m-temperature. Note: relative humidity has a different colour bar for 12.5 km and 3 km grid resolution.

3.2. Climate change related impacts across grid resolutions: Influenza, pollen, mold

The impact cases, influenza, pollen, and mold, aim to demonstrate the difference and potentially the added value on the 3 km grid resolution, compared to the 12.5 km grid resolution, to simulate climate change impacts in the Berlin region. The following results reveal how the defined meteorological conditions change for each impact case under near-term climate change for Berlin and its surroundings.

3.2.1. Less influenza days per year, but longer periods of consecutive influenza days

The REMO model outcomes show that the influenza days, happening from December to March with a day mean of SH < 0.006 kg/kg and temperatures between 2– 6 °C, will decrease under the considered future climate conditions, comparing the near-term period 2041–2050 with the historical period 1996–2005 (Fig. 5). However, the duration of periods with consecutive influenza days are projected to become longer in the considered future decade (Fig. 6).

A stronger change signal is found for the 3 km resolution, with a decrease of −2 influenza d/yr compared to around −1 influenza d/yr for the 12.5 km resolution for the future period, for both Berlin and its surroundings (Fig. 5, Appendices: Table A3). The decrease in influenza days in the near-term future period could be explained by overall warmer temperatures under climate change, resulting in a smaller amount of cold days in the winter (e.g. Brasseur et al., 2017). The warmer temperatures could lead to higher humidity levels, as warm air can hold more moisture. This is also in line with Langendijk et al. (2019), who indicate specific humidity increases under future climate change (RCP8.5) throughout the 21st century in the Berlin region. The stronger decrease of influenza days on the 3 km

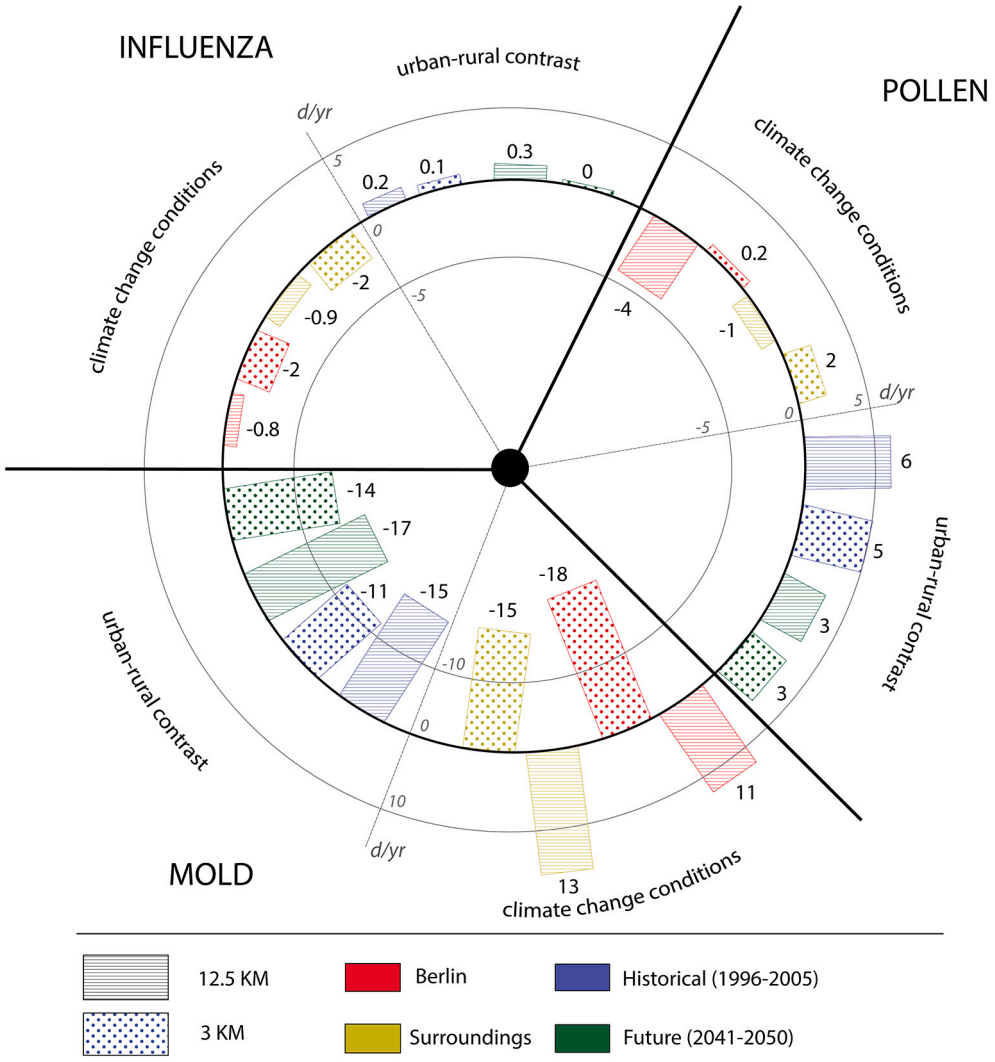

Fig. 5. Mean change in days per year (d/yr) for each impact case: influenza; pollen; and mold. Showing the grid resolutions (3 km and 12.5 km), under near-term future climate conditions vs. historic climate conditions (= future (2041– 2050) - historical (1996– 2005) and urban-rural contrast (= Berlin - surroundings) (see Appendices: Table A3).

resolution may be a result of the convection-permitting scale, which tends to have slightly higher specific humidity levels than the 12.5 km resolution, particularly in the winter months, as shown in Fig. 3 and Fig. 4.

Uninterrupted periods of consecutive influenza days occur in the historical period with an average duration between 2– 8 consecutive days (Fig. 6, interquartile range), with a median of 4 days for all time slices and resolutions, and extreme periods up to 50 consecutive influenza days (Fig. 6). Fig. 6 indicates that the duration of the periods with consecutive influenza days will increase under near-term future climate change, especially for the 3 km resolution, by ~~2~~ 3 consecutive days (expansion of upper quartile (Q3) of boxplot). This is shown in Fig. 6 by the interquartile range change from 2 – 8 to 2 – 10 consecutive influenza days for Berlin under near-term climate change.

The model evaluation indicates that the REMO model on the 3 km resolution better simulates specific humidity (Pearson correlation coefficient) and temperature (RMSE, and/or MBE, and/or Pearson) during the months December – March. Despite a relatively small difference between the 3 km and 12.5 km resolution, it is expected that the convection-permitting scale may bring about more reliable results for the influenza impact case.

The urban-rural contrast is minimal for influenza, with a 0 – 0.3 d/yr difference between Berlin and its surroundings (Fig. 5,

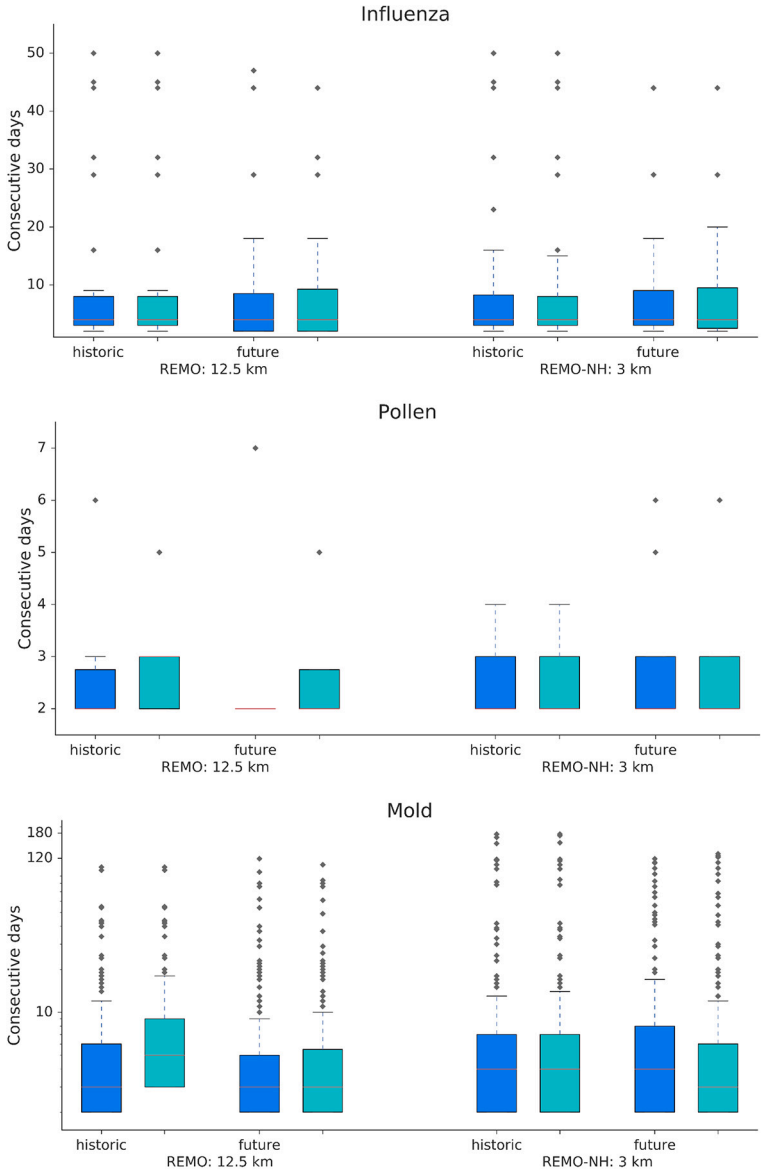

Fig. 6. Boxplots showing the consecutive days for each impact case: influenza; pollen; and mold. For Berlin (blue) and its surroundings (green), for the grid resolutions (12.5 km (left) and 3 km (right)), for historical (1996– 2005) and near-term future (2041– 2050) period. Boxplots: the model median (red line), quartiles (Q1: 25% and Q3: 75%), and whiskers (1.5 * IQR (IQR = Q3 - Q1)) indicate the model spread. (For interpretation of the references to colour in this figure legend, the reader is referred to the web version of this article.)

Table A3
Change in days per year for the grid resolutions (3 km and 12.5 km), for climate change (future – historical) and urban-rural contrast (Berlin – surroundings).

		Climate change *(future - historical)*			Urb-rur contrast *(Berlin - surr)*	
		12.5 km	3 km		historical	future
Influenza	*Berlin*	−1	−2	*12.5 km*	+0.2	+0.3
	Surroundings	−1	−2	*3 km*	+0.1	0
Pollen	*Berlin*	−4	+0,2	*12.5 km*	6	3
	Surroundings	−1	2	*3 km*	5	3
Mold	*Berlin*	11	−18	*12.5 km*	−15	−17
	Surroundings	13	−15	*3 km*	−11	−14

Appendices: Table A3). This is in line with observations and model outcomes for the winter months for specific humidity (Fig. 3).

3.2.2. More pollen days on the convection-permitting scale, and in Berlin, under future climate conditions

There is an increase in pollen days, characterized by a day mean of RH < 60% in July – October, simulated under future climate conditions on the 3 km resolution, especially in Berlin compared to its surroundings (Fig. 5). Notably, the 12.5 km resolution indicates a decrease of −4 d/yr in Berlin and − 1 d/yr for its surroundings in the future period 2041– 2050, in contrast to an increase of 0.2 d/yr in Berlin and 2 d/yr in the surroundings for the 3 km resolution. There is a sign change for the change signal going from the 12.5 km to the convection-permitting resolution. Following previous literature, an increase in pollen days under climate change is expected, especially in Berlin, because it would become hotter and less moist in the city, especially in the summer months (Argüeso et al., 2014; Langendijk et al., 2019; Lin et al., 2020; Lokoshchenko, 2017; Zhao et al., 2021). Taking this into consideration, the convention permitting resolution behaves closer to the expectations. This is probably the case because REMO-NH better resolves the urban surface, and therefore better simulates the drier and warmer urban conditions and the urban dry island effect in the summer, compared to the 12.5 km resolution (Table 1). This is in line with the statistical improvements found for the 3 km grid resolution for the RH urban-rural difference (Fig. 3, Appendices: Table A1). Therefore, an added value for the convection-permitting scale is detected to simulate the pollen impact case.

There is a large urban-rural contrast, with more pollen days in Berlin, for both the 12.5 km and 3 km grid resolutions, ranging from 5–6 d/yr in the historical period and 3 d/yr in the future period. The urban-rural difference for relative humidity is also clearly visible on the spatial maps (Fig. 4), and is more detailed for the 3 km resolution. This overall result is expected, as Berlin is generally less moist than its surroundings, resulting in more pollen days in the city (Langendijk et al., 2019; Zhao et al., 2021). The decrease of the urban-rural contrast in the future period compared to the historical period can be explained by the relative increase of pollen days in the surroundings, for the 3 km grid resolution. For the 12.5 km grid resolution the pollen days show a stronger relative decrease in Berlin, compared to the surroundings.

The periods of consecutive pollen days range from 2 – 3 days, with extremes up to 7 days. No major difference is found for the consecutive pollen days under future climate conditions, nor for the different resolutions in this respect.

3.2.3. Less mold days on the convection-permitting resolution, but longer consecutive periods, under future climate conditions

Mold days, defined by a day mean of RH >80% and temperatures between 10 – 40 °C, will become less under near-term climate conditions on the 3 km resolution for the Berlin region (Fig. 5). Nevertheless, the periods of consecutive mold days become longer for the future period 2041– 2050, especially on the convection-permitting resolution (Fig. 6).

Worth noting is the sign change of the change signal going from the 12.5 km to the 3 km grid resolution (Fig. 5). An increase of 11 (Berlin) – 13 (surroundings) mold d/yr is found for the 12.5 km resolution for the future time period, in contrast to the 3 km resolution, which shows a decrease of 18 (Berlin) – 15 (surroundings) mold d/yr under near-term climate change conditions (Fig. 5, Appendices: Table A3). Following previous literature, mold days are expected to decrease under climate change, especially in Berlin in the summer. It will become warmer, and relative humidity decreases particularly in the urban area, as there is little moisture available in the city to be added to the atmosphere (Argüeso et al., 2014; Langendijk et al., 2019; Lokoshchenko, 2017; Zhao et al., 2021). This leads to the conclusion, that the convection-permitting scale (REMO-NH) better resolves the urban surface, leading to warmer temperatures and reduced relative humidity, especially in Berlin, resulting in less mold days under near-term climate conditions. A clear added value on the convection-permitting scale is identified for simulating mold days in an urban-rural context, similar to the pollen impact case.

Longer periods of consecutive mold days are projected for the 3 km and 12.5 km resolution under future climate conditions. The period of consecutive mold days generally ranges between 2–8 days, with extremes up to 170 consecutive days (Fig. 6). The median shifts from 3 to 4 consecutive days for the 3 km resolution. This is a critical change, as prior research shows that indoor mold growth strongly increases after four consecutive mold days (Sedlbauer, 2001). In addition, the upper quartile (Q2) increases for the future, especially on the convection-permitting resolution, making longer consecutive mold periods more likely.

Berlin has −15 mold d/yr less than its surroundings on the 12.5 km resolution, and − 11 d/yr on the 3 km grid resolution, for the historical period. An even larger urban-rural contrast is found for the future period with Berlin showing less mold days than its surroundings by −17 d/yr on the 12.5 km and − 14 d/yr on the 3 km resolution (Fig. 5). This urban-rural difference is also clearly visible on the spatial maps (Fig. 4), and is more detailed on the 3 km resolution. Berlin is expected to be less moist than its surroundings and therefore experiencing less mold days. This gets larger under climate change, as the city get drier (RH) and warmer, and its surroundings might have more capacity to add additional moisture to the atmosphere when warming (Langendijk et al., 2019; Zhao et al., 2021).

In summary, the 3 km grid resolution, the convection-permitting scale, improves the simulations for the impact cases in the Berlin region, compared to the 12.5 km grid resolution. This influences the results for influenza, leading to a more profound decrease of influenza days under future climate conditions. A sign change of the change signal is identified for the 3 km compared to the 12.5 km grid resolution for the impact cases pollen, and mold, showing an increase in pollen days and a decrease in mold days under near-term climate conditions. There is an added value detected on the convection-permitting resolution to simulate the climate change impact cases.

4. Discussion and conclusions

The outcomes of this research confirm that the convection-permitting resolution better resolves regional-to-local scales, for complex terrains such as urban areas (Argüeso et al., 2016; Coppola et al., 2020; Kendon et al., 2021; Prein et al., 2015). Improved urban detail is found (Fig. 4), as well as a stronger change signal for influenza, and a sign change of the change signal for the pollen and mold impact case, moving from the 12.5 km to the 3 km grid resolution. The model evaluation and the pollen case indicate that particular added value is found in the summer months, which is in line with other literature that show improvements particularly in this season (Ban et al., 2014; Kendon et al., 2021; Prein et al., 2015). This may be particularly true for Berlin, as the simple urban scheme may better capture the heat retention and related urban moist reduction in the summer months (Fig. 3, Table 2), compared to the winter months. The urban scheme does not include anthropogenic heat, which may be one of the key reasons that the model underestimates the temperature and urban moist reduction in the winter (Jin et al., 2021).

The results show little improvement for the annual mean values for the 3 km grid resolution. This is in contrast to the added value found on a monthly basis for the annual cycle. The REMO-NH model at 3 km resolution shows improved statistical outcomes for specific months for temperature, and to a less extent for relative and specific humidity, as well as for the meteorological conditions of the impact cases, and the RH urban-rural contrast. This is in line with e.g. Argüeso et al. (2016) and Prein et al. (2015), who show that the convection-permitting scale mainly shows added value on shorter timescales, rather than for annual means (Ban et al., 2014; Kendon et al., 2021).

This study relies on one model and one decade under near term future climate conditions using the RCP8.5 scenario. The outcomes are model depended and only reflect one possible future, for one future decade. Therefore, similar studies with different models and under different climate change scenarios are needed, in order to compare and validate the results of this study (Coppola et al., 2020; Fosser et al., 2020). In conjunction, only the near-term period is investigated for climate change impacts. The changes for the impact cases may look different for the far future, e.g. up to 2100. Additionally, comparing historic periods with future periods with a minimal duration of 20- 30 years would be needed to distill a robust climate change signal and/or the climate change effect on the impact cases. To adequately assess the impact cases under longer term climate change, transient high-resolution climate change simulations would be preferred.

Despite the added value found for the 3 km grid resolution in this study, it is crucial to further reflect if the change signal is more trustworthy on the convection-permitting scale, and which change signals can be reliably captured by courser-resolution models (Fosser et al., 2020; Kendon et al., 2021). Although, this research implies that for the pollen and mold impact case the 3 km resolution is showing a more reliable sign of the change signal, robustness shall be further assessed using other models and approaches, as well as longer time periods up to 20 to 30 years (Hawkins et al., 2020; IPCC, 2013). The change in the sign may trigger a difference in the response by decision makers from inaction to action. Here, the challenge arises how to best communicate the divergent results stemming from the 12.5 km and 3 km grid resolution, especially to urban planners and decision makers (Kendon et al., 2021).

In addition, the results on the 3 km show clear improvements, but also highlight that the effect of the urban parametrization is no longer negligible at this grid resolution (Argüeso et al., 2016; Trusilova et al., 2013). Sophisticated urban models have greater complexity and are able to simulate fine scale meteorological processes and fluxes in the city and on the district, or even building level. Sophisticated urban schemes could improve the simulation of the urban local-to-regional interactions, e.g. the overestimation of relative humidity in the winter, and the overestimation of the SH urban-rural contrast in summer (Daniel et al., 2019). It would be important to consider incorporating anthropogenic heat in the winter. This study calculates averaged values over Berlin, to understand mean changes for the city compared to its surrounding. Nevertheless, local conditions may affect the impact cases significantly, which needs to be investigated with more sophisticated urban models.

4.1. Implications for the impact cases

The results of this research show a stronger decrease of influenza days on the convection-permitting scale under near-term future climate conditions (2041– 2050), but consecutive periods become longer particularly on the 3 km grid resolution. The longer influenza periods might enhance spreading and the survival of the virus and could increase the related infections and therefore hospitalizations, in line with e.g. Chong et al. (2020). Generally, projected warmer and moister winters under climate change could potentially lead to a decrease in influenza. Though, other research shows that a warmer winter might spark an enhanced influenza pandemic with early onset the subsequent year when it is colder and/or less moist (Towers et al., 2013). Further research is needed to investigate seasonal cycles, extremes, and match them with further relevant factors to understand the interactions with climate change (Chong et al., 2020; Goodwins et al., 2019).

Higher amounts of pollen days are simulated on the 3 km grid resolution, especially in Berlin, under near-term future climate conditions. The increase of pollen days on the convection-permitting resolution coincides with the estimation by Hamaoui-Laguel et al. (2015) that by 2050 airborne ragweed pollen concentrations will be about four times higher than they are now in Europe. In addition, climate change could increase the length and severity of the pollen season and, as a consequence, the associated pollen allergy (D'Amato and Cecchi, 2008; Ziska et al., 2003). Ragweed is expected to expand its range due to climate change in Europe, particularly in the Northern parts of the continent (Cunze et al., 2013; Storkey et al., 2014). In this context, the sign change of the change signal on the convection-permitting scale is therefore of particular relevance, as the increase in pollen days coincides with other climate change effects on ragweed pollen prevalence. Urban planners and decision makers shall take people suffering from pollen allergy into account when planting in public spaces (Bergmann et al., 2012). To prevent the further spread of ragweed, the plants shall be systematically registered and destroyed (Buters et al., 2015; Pflanzenschutzamt Berlin, 2021).

A decrease in the amount of mold days/year for the near-term period are expected on the 3 km grid resolution, but the consecutive periods might get longer. This finding is in line with Bertolin and Camuffo (2014), who show a decrease for a relatively similar indicator "Time of wetness" (RH $>$ 85%, and temperatures $>$0 °C), under RCP4.5 in the Berlin region. Despite this overall decrease, the longer periods of consecutive mold days, may imply more indoor mold growth. Particularly the shift in the median from 3 to 4 consecutive days in the future, may enhance indoor mold growth, as this is a critical threshold for mold growth shown by studies from Sedlbauer (2001) and Viitanen and Ojanen (2007). Climate change may lead to warmer winters and prolonged mild temperatures between fall and spring. This could provide improved mold growth conditions and lengthen the optimal mold growth period. Other studies also found possible increases in indoor mold growth under climate change (Huijbregts et al., 2012; Leissner et al., 2015). These studies focus on specific, vulnerably buildings, using sophisticated building models and by constructing a mold index on various variables. Further coupling the climate projections used in this research to building models at specific locations might change the results. More detailed models and follow up studies would be helpful to understand the climate change effects for specific buildings, streets, or a neighborhood.

The impact cases are designed around humidity thresholds, and their simulated changes under near-term future climate conditions. Other factors have not been directly taken into account that could influence the outcomes of the impact cases, and the potential effects on human health.

For instance, for influenza, it would be important to further simulate and understand the role of changes in human behavior, the susceptibility to the virus of city dwellers, the indoor temperature and humidity, as well as to better understand how the effect would be different in other climate regimes (e.g. tropics) (Davis et al., 2016; Deyle et al., 2016). Dalziel et al. (2018) investigated 603 cities in the United States of America (USA) to understand the connection between urbanization and influenza. Influenza epidemics in smaller cities are shorter and strongly linked to humidity fluctuations. Whereas in larger cities non-climate factors have a more profound influence and a milder response to climate factors is found. Outdoor, as well as indoor, air pollution are associated with higher influenza incidence, and increased severity of the health risks related to the virus, particularly in winter months with low temperatures (Meng et al., 2021; Murtas and Russo, 2019; Song et al., 2021; Su et al., 2019; Toczylowski et al., 2021; Wang et al., 2016). Studies show a positive association between higher influenza risks and people who suffer from asthma as well as other respiratory allergies, obesity, or are recipient of a treatment for a chronic disease (Guerrisi et al., 2019; Hirota et al., 1992; Jain and Chaves, 2011; Karki et al., 2018; Yang et al., 2013). Prior studies show lifestyle choices, such as smoking enhance influenza risks (Choi et al., 2014; Guerrisi et al., 2019; Wong et al., 2013). In contrast, regular exercise and healthy diets counter health risks associated with influenza (Hirota et al., 1992; Wong et al., 2013). Certain studies indicate that women are more prone to influenza risks (Guerrisi et al., 2019; WHO, 2010). Particularly, the severity of the disease is worse among pregnant women (WHO, 2010). In this context, it is important to take into account that the rate of exposure to influenza could be higher for women than man, because they more often are caregivers and/or work in health-care occupations (WHO, 2010).

For the pollen impact case, it would be crucial to understand the quantity of ragweed plants in the city and how many allergic people live in the city (D'Amato and Cecchi, 2008). Urban environments provide beneficial growing conditions for ragweed mainly due to higher temperatures and CO2 emissions (Cvetkovski et al., 2018; Deutschewitz et al., 2003). Simultaneously, the high levels of air pollution in cities worsen pollen allergies of its inhabitants (Leru et al., 2021; Sedghy et al., 2018), with ozone being the most

inflammatory pollutant (Kay et al., 2020). On another note, Voros et al. (2018) show that parents with the genetic tendency to develop allergic diseases (atopy) have children that develop pollen allergies more frequently (Voros et al., 2018). Also, smokers are more likely to suffer from allergy symptoms (Leru et al., 2021). Kusunoki et al. (2017) investigated 520 children at an age of 10, and found that the sensitization rate to ragweed was significantly decreased with increases in fruit intake. This hinds at diet choices might even influence the severity of ragweed pollen allergies.

For the mold impact case, the substrate and the indoor climate are pivotal to further understand the mold growth in the building (Ojanen et al., 2010; Ritschkoff et al., 2000; Sedlbauer, 2001; Viitanen and Ojanen, 2007). Indoor mold growth has been associated in many studies with an increased risk and amplification of asthma and respiratory illness (Hurraß et al., 2017; Mendell and Kumagai, 2017; Seguel et al., 2017; Sinclair et al., 2018). There is some evidence mold exposure leads to lower lung function, dermatitis, and non-respiratory symptoms (e.g. eye symptoms, headache, fatigue) (Norbäck, 2020). Particularly, moldy work and home environments are known to raise the exposure rate, and respectively the related health risks (Dales et al., 1991; Hurraß et al., 2017). In Germany, mold damage is found in every 10th home (Wiesmüller et al., 2016). Studies for the United States of America indicate higher asthma prevalence and related morbidity for Black and Latinx communities than for White Americans, directly associated with the higher levels of mold contamination in their homes (Grant et al., 2022; Sinclair et al., 2018). This indicates that racial/ethnic/social inequities may enhance the health risks in connection with indoor mold growth (Grant et al., 2022).

Interdisciplinary research shall be undertaken to better understand the interaction between the changing climate and other critical non-climatic factors that influence the health related aspects of each impact case.

4.2. Concluding remarks

Concluding, the convection-permitting scale, improves the simulations for the impact cases, influenza, pollen, and mold in the Berlin region, compared to the 12.5 km grid resolution. This is one of the first studies that explores these impact cases under future climate conditions in the urban-rural context, with convection-permitting models. Influenza shows a more profound decrease of influenza days on the convection-permitting scale under future climate conditions, but longer consecutive periods especially on the 3 km grid resolution. A difference in the sign of the change signal is identified for the 3 km compared to the 12.5 km grid resolution for the impact cases pollen, and mold. The convection-permitting resolution performs more in line with observations, and available literature on urban processes, showing an increase in pollen days and a decrease in mold days under near-term climate conditions. The pollen days are more prevalent in Berlin. Mold periods are projected to increase in its duration under near-term climate conditions, showing a stronger increase on the 3 km grid resolution. The convection-permitting resolution affects, and generally improves the outcomes for the impact cases, and shows an added value, indicating the potential of convection-permitting simulations to generate improved information about climate change impacts for urban areas and its surroundings. This is of importance for the development of climate services for urban areas, as the improved information could enable urban planners and decision makers to more adequately prepare for and adapt to future climate change impacts.

CRediT authorship contribution statement

Gaby S. Langendijk: Conceptualization, Data curation, Formal analysis, Investigation, Methodology, Validation, Visualization, Writing – original draft, Writing – review & editing. **Diana Rechid:** Conceptualization, Supervision, Writing – review & editing. **Daniela Jacob:** Conceptualization, Supervision, Writing – review & editing.

Declaration of Competing Interest

The authors declare that they have no known competing financial interests or personal relationships that could have appeared to influence the work reported in this paper.

Acknowledgements

We wish to thank the European Climate Prediction (EUCP) project (EU H2020 project Grant agreement: 776613) for making the data available enabling this research, and particularly dr. Thomas Frisius for providing the data. The research was kindly funded by the Climate Service Center Germany (GERICS), Helmholtz-Zentrum Hereon, Germany. We kindly thank our colleague dr. Laurens Bouwer for providing constructive feedback on the first version of the manuscript.

Appendices

Fig. A1. Locations of the observational stations in Berlin and its surroundings.

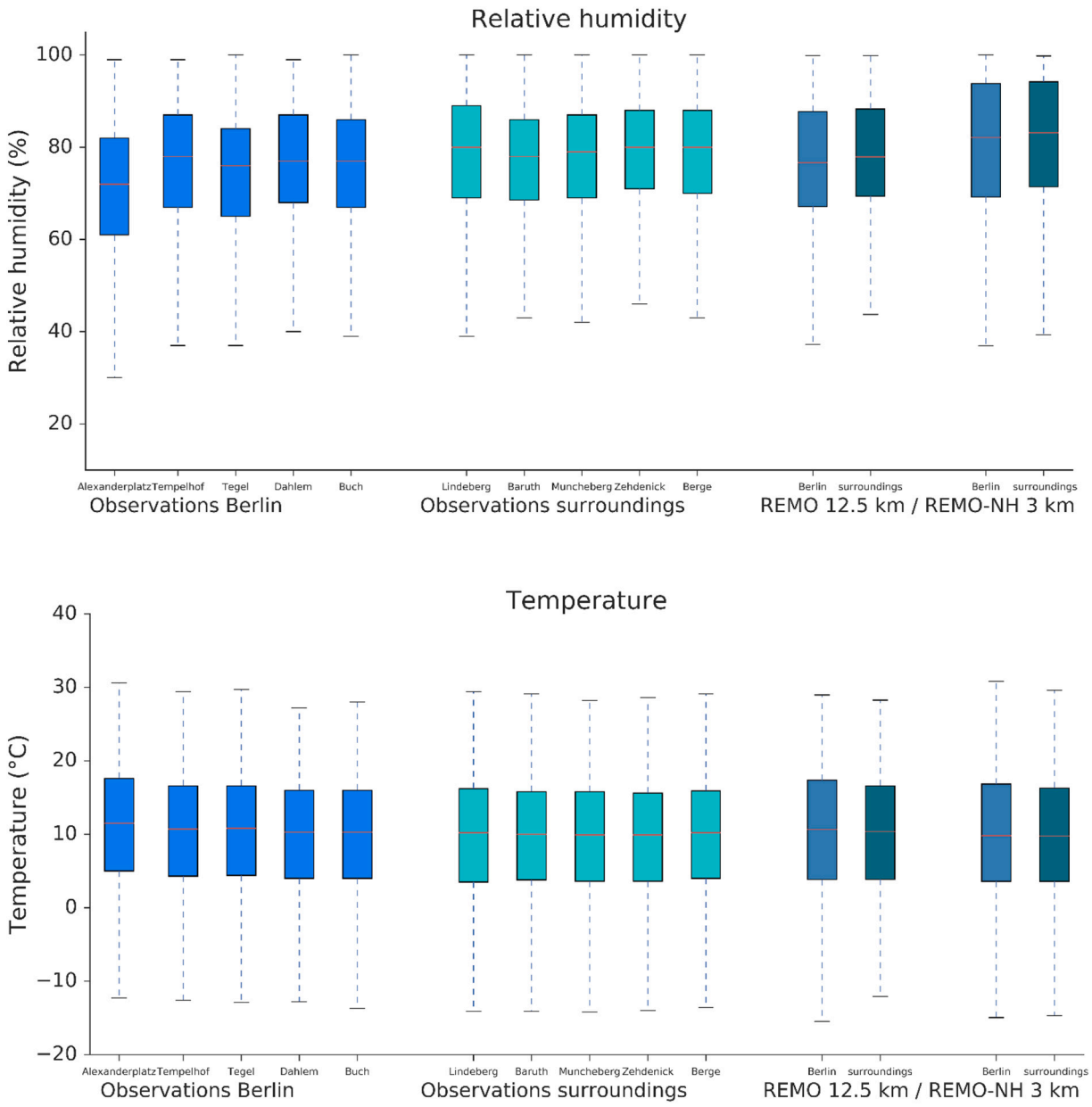

Fig. A2. *Boxplots show the averaged day mean of observational station data for relative humidity and 2-m temperature, for the period 2000– 2009 , for Berlin and its surroundings. REMO model data averaged for the same period 2000– 2009 is presented on right side of figure, respectively for REMO 12.5 km and REMO-NH 3 km grid resolutions.*

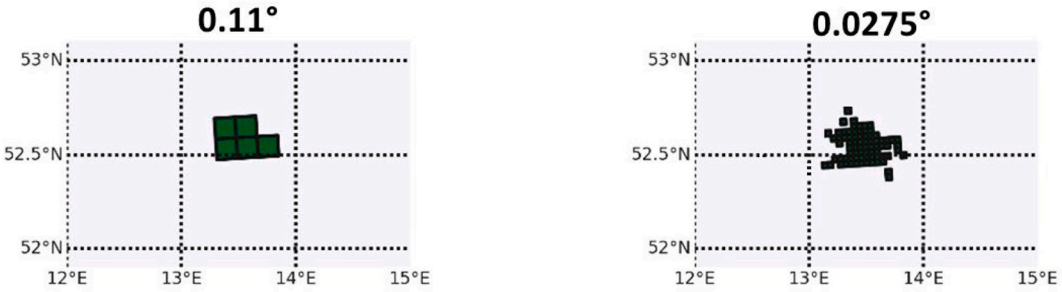

Fig. A3. Masks for Berlin, based on urban fraction >0.3, for 12.5 km (0.11°, left) and 3 km (0.0275°, right) grid resolutions.

Table A1
RMSE, MBE and Pearson correlation coefficient for relative humidity, specific humidity, and temperature, day mean 2000– 2009, for Berlin comparing observations with the 12.5 km and 3 km grid resolution. Calculated the mean over the 10 years per day.

	Berlin 12.5 km	Berlin 3 km	Surroundings 12.5 km	Surroundings 3 km	Urb-rur contrast 12.5 km	Urb-rur contrast 3 km	Obs Berlin vs Obs Surr
Relative Humidity							
RMSE (%):	5.57	9.50	4.49	7.73	2.43	2.29	3.29
MBE (%):	-2.58	-6.34	-0.81	-4.43	-1.77	-1.91	-3.16
Pearson corr.:	0.85	0.73	0.85	0.74	0.22	0.24	0.996
Specific Humidity							
RMSE (kg/kg):	0.00074	0.00078	0.00121	0.00128	0.00053	0.00060	0.00009
MBE (kg/kg):	-0.00052	-0.00065	-0.00085	-0.00102	0.00033	0.00038	-0.00004
Pearson corr.:	0.984	0.983	0.9803	0.9796	0.653	0.635	0.999
2-m Temperature							
RMSE (°C):	1.01	1.02	0.93	0.88	0.51	0.57	0.71
MBE (°C):	-0.11	0.25	-0.43	-0.19	0.32	0.44	0.69
Pearson corr.:	0.99	0.99	0.99	0.99	0.20	0.21	0.9998

Table A2
Standard deviation for day mean over 2000–2009 for specific humidity, relative humidity (also hourly mean 2000–2009) for observations, 12.5 km and 3 km grid resolutions, for Berlin and its surroundings.

	Obs Berlin	*Berlin 12.5 km*	*Berlin 3 km*	*Obs Surroundings*	*Surroundings 12.5 km*	*Surroundings 3 km*
Relative humidity (%)	8.56	9.15	10.21	8.03	7.86	9.25
Specific humidity (kg/kg)	0.00213	0.00246	0.00227	0.00216	0.00286	0.00275

References

Amt für Statistik Berlin-Brandenburg, 2020. Statistiken Berlin und Brandenburg [WWW Document]. Statistiken. URL. https://www.statistik-berlin-brandenburg.de/statistiken/Inhalt-Statistiken.asp (accessed 7.26.19).

Argüeso, D., Evans, J.P., Fita, L., Bormann, K.J., 2014. Temperature response to future urbanization and climate change. Clim. Dyn. https://doi.org/10.1007/s00382-013-1789-6.

Argüeso, D., Di Luca, A., Evans, J.P., 2016. Precipitation over urban areas in the western maritime continent using a convection-permitting model. Clim. Dyn. 47, 1143–1159. https://doi.org/10.1007/s00382-015-2893-6.

Bai, X., Dawson, R.J., Ürge-Vorsatz, D., Delgado, G.C., Salisu Barau, A., Dhakal, S., Dodman, D., Leonardsen, L., Masson-Delmotte, V., Roberts, D.C., Schultz, S., 2018. Six research priorities for cities and climate change. Nature. https://doi.org/10.1038/d41586-018-02409-z.

Baklanov, A., Grimmond, C.S.B., Carlson, D., Terblanche, D., Tang, X., Bouchet, V., Lee, B., Langendijk, G., Kolli, R.K., Hovsepyan, A., 2018. From urban meteorology, climate and environment research to integrated city services. Urban Clim. 23 https://doi.org/10.1016/j.uclim.2017.05.004.

Ban, N., Schmidli, J., Schär, C., 2014. Evaluation of the convection-resolving regional climate modeling approach in decade-long simulations. J. Geophys. Res. 119, 7889–7907. https://doi.org/10.1002/2014JD021478.

Ban, N., Caillaud, C., Coppola, E., Pichelli, E., Sobolowski, S., Adinolfi, M., Ahrens, B., Alias, A., Anders, I., Bastin, S., Belušić, D., Berthou, S., Brisson, E., Cardoso, R. M., Chan, S.C., Christensen, O.B., Fernández, J., Fita, L., Frisius, T., Gašparac, G., Giorgi, F., Goergen, K., Haugen, J.E., Hodnebrog, Ø., Kartsios, S., Katragkou, E., Kendon, E.J., Keuler, K., Lavin-Gullon, A., Lenderink, G., Leutwyler, D., Lorenz, T., Maraun, D., Mercogliano, P., Milovac, J., Panitz, H.J., Raffa, M., Remedio, A. R., Schär, C., Soares, P.M.M., Srnec, L., Steensen, B.M., Stocchi, P., Tölle, M.H., Truhetz, H., Vergara-Temprado, J., de Vries, H., Warrach-Sagi, K., Wulfmeyer, V., Zander, M.J., 2021. The first multi-model ensemble of regional climate simulations at kilometer-scale resolution, part I: evaluation of precipitation. Clim. Dyn. https://doi.org/10.1007/s00382-021-05708-w.

Barreca, A.I., Shimshack, J.P., 2012. Absolute humidity, temperature, and influenza mortality: 30 years of county-level evidence from the United States. Am. J. Epidemiol. https://doi.org/10.1093/aje/kws259.

Beest, D.E.T., Van Boven, M., Hooiveld, M., Van Den Dool, C., Wallinga, J., 2013. Driving factors of influenza transmission in the Netherlands. Am. J. Epidemiol. 178, 1469–1477. https://doi.org/10.1093/aje/kwt132.

Bergmann, K.-C., Zuberbier, T., Augustin, J., Mücke, H.-G., Straff, W., 2012. Klimawandel und Pollenallergie: Städte und Kommunen sollten bei der Bepflanzung des öffentlichen Raums Rücksicht auf Pollenallergiker nehmenClimate change and pollen allergy: In the plantation of public spaces, cities and municipalities should take into a. Allergo J. 21, 103–108. https://doi.org/10.1007/s15007-012-0045-4.

Bertolin, C., Camuffo, D., 2014. Climate change impact on movable and immovable cultural heritage throughout Europe. Climate for Culture, Deliverable 5.

Bianchi, D.E., Schwemmin, D.J., Wagner, W.H., 1959. Pollen release in the common ragweed (Ambrosia artemisiifolia). Bot. Gaz. https://doi.org/10.1086/336030.

Brasseur, G.P., Jacob, D., Schuck-Zöller, S., 2017. Klimawandel in Deutschland: Entwicklung, Folgen, Risiken und Perspektiven. Chemie in Unserer Zeit.

Bundesministerium für Raumordnung, B. und S., 1995. Dritter_Bericht_ueber_Schaeden_an_Gebaeuden_1995_.pdf.

Buters, J., Alberternst, B., Nawrath, S., Wimmer, M., Traidl-Hoffmann, C., Starfinger, U., Behrendt, H., Schmidt-Weber, C., Bergmann, K.-C., 2015. Ambrosia artemisiifolia (ragweed) in Germany – current presence, allergological relevance and containment procedures. Allergo J. Int. 24, 108–120. https://doi.org/10.1007/s40629-015-0060-6.

Caini, S., Spreeuwenberg, P., Donker, G., Korevaar, J., Paget, J., 2018. Climatic factors and long-term trends of influenza-like illness rates in the Netherlands, 1970–2016. Environ. Res. https://doi.org/10.1016/j.envres.2018.07.035.
Choi, S.M., Jeong, Y.-J., Park, J.S., Kang, H.J., Lee, Y.J., Park, S.S., Lim, H.-J., Chung, H.S., Lee, C.-H., 2014. The impact of lifestyle behaviors on the acquisition of pandemic (H1N1) influenza infection: a case-control study. Yonsei Med. J. 55, 422–427.
Chong, K.C., Lee, T.C., Bialasiewicz, S., Chen, J., Smith, D.W., Choy, W.S.C., Krajden, M., Jalal, H., Jennings, L., Alexander, B., Lee, H.K., Fraaij, P., Levy, A., Yeung, A. C.M., Tozer, S., Lau, S.Y.F., Jia, K.M., Tang, J.W.T., Hui, D.S.C., Chan, P.K.S., 2020. Association between meteorological variations and activities of influenza a and B across different climate zones: a multi-region modelling analysis across the globe. J. Inf. Secur. 80, 84–98. https://doi.org/10.1016/j.jinf.2019.09.013.
Coppola, E., Sobolowski, S., Pichelli, E., Raffaele, F., Ahrens, B., Anders, I., Ban, N., Bastin, S., Belda, M., Belusic, D., Caldas-Alvarez, A., Cardoso, R.M., Davolio, S., Dobler, A., Fernandez, J., Fita, L., Fumiere, Q., Giorgi, F., Goergen, K., Güttler, I., Halenka, T., Heinzeller, D., Hodnebrog, Jacob, D., Kartsios, S., Katragkou, E., Kendon, E., Khodayar, S., Kunstmann, H., Knist, S., Lavín-Gullón, A., Lind, P., Lorenz, T., Maraun, D., Marelle, L., van Meijgaard, E., Milovac, J., Myhre, G., Panitz, H.J., Piazza, M., Raffa, M., Raub, T., Rockel, B., Schär, C., Sieck, K., Soares, P.M.M., Somot, S., Srnec, L., Stocchi, P., Tölle, M.H., Truhetz, H., Vautard, R., de Vries, H., Warrach-Sagi, K., 2020. A first-of-its-kind multi-model convection permitting ensemble for investigating convective phenomena over Europe and the Mediterranean. Clim. Dyn. https://doi.org/10.1007/s00382-018-4521-8.
Cunze, S., Leiblein, M.C., Tackenberg, O., 2013. Range expansion of Ambrosia artemisiifolia in Europe is promoted by climate change. ISRN Ecol. 2013, 1–9. https://doi.org/10.1155/2013/610126.
Curtis, R., 2010. Climate change and traditional buildings: the approach taken by historic Scotland. J. Archit. Conserv. https://doi.org/10.1080/13556207.2010.10785073.
Cvetkovski, B., Kritikos, V., Yan, K., Bosnic-Anticevich, S., 2018. Tell me about your hay fever: a qualitative investigation of allergic rhinitis management from the perspective of the patient. NPJ Prim. Care Respir. Med. 28, 1–7.
Dales, R.E., Zwanenburg, H., Burnett, R., Franklin, C.A., 1991. Respiratory health effects of home dampness and molds among Canadian children. Am. J. Epidemiol. 134, 196–203. https://doi.org/10.1093/oxfordjournals.aje.a116072.
Dalziel, B.D., Kissler, S., Gog, J.R., Viboud, C., Bjørnstad, O.N., Metcalf, C.J.E., Grenfell, B.T., 2018. Urbanization and humidity shape the intensity of influenza epidemics in U.S. cities. Science (80-.). 362, 75–79. https://doi.org/10.1126/science.aat6030.
D'Amato, G., Cecchi, L., 2008. Effects of climate change on environmental factors in respiratory allergic diseases. Clin. Exp. Allergy. https://doi.org/10.1111/j.1365-2222.2008.03033.x.
Daniel, M., Lemonsu, A., Déqué, M., Somot, S., Alias, A., Masson, V., 2019. Benefits of explicit urban parameterization in regional climate modeling to study climate and city interactions. Clim. Dyn. 52 (5), 2745–2764. https://doi.org/10.1007/s00382-018-4289-x.
Davis, R.E., McGregor, G.R., Enfield, K.B., 2016. Humidity: a review and primer on atmospheric moisture and human health. Environ. Res. 144, 106–116. https://doi.org/10.1016/j.envres.2015.10.014.
Deutschewitz, K., Lausch, A., Kühn, I., Klotz, S., 2003. Native and alien plant species richness in relation to spatial heterogeneity on a regional scale in Germany. Glob. Ecol. Biogeogr. 12, 299–311.
Deyle, E.R., Maher, M.C., Hernandez, R.D., Basu, S., Sugihara, G., 2016. Global environmental drivers of influenza. Proc. Natl. Acad. Sci. U. S. A. https://doi.org/10.1073/pnas.1607747113.
Di Luca, A., de Elía, R., Laprise, R., 2015. Challenges in the quest for added value of regional climate dynamical downscaling. Curr. Clim. Chang. Rep. https://doi.org/10.1007/s40641-015-0003-9.
Dingle, A.N., Gill, G.C., Wagner, W.H., Hewson, E.W., 1959. The emission, dispersion, and deposition of ragweed pollen. Adv. Geophys. https://doi.org/10.1016/S0065-2687(08)60123-5.
DWD, D., 2021. German Weather Service, Climate Data Center (CDC) [WWW Document]. URL. https://cdc.dwd.de/portal/ (accessed 5.8.21).
EEA, 2000. The Revised and Supplemented Corine Land Cover Nomenclature. EEA Tech. Rep. No 40.
Fosser, G., Kendon, E.J., Stephenson, D., Tucker, S., 2020. Convection-permitting models offer promise of more certain extreme rainfall projections. Geophys. Res. Lett. https://doi.org/10.1029/2020GL088151.
Fuhrmann, C., 2010. The effects of weather and climate on the seasonality of influenza: what we know and what we need to know. Geogr. Compass 4, 718–730. https://doi.org/10.1111/j.1749-8198.2010.00343.x.
Ghiani, A., Ciappetta, S., Gentili, R., Asero, R., Citterio, S., 2016. Is ragweed pollen allergenicity governed by environmental conditions during plant growth and flowering? Sci. Rep. 6 https://doi.org/10.1038/srep30438.
Goettel, H., 2009. Einfluss der nichthydrostatischen Modellierung und der Niederschlagsverdriftung auf die Ergebnisse regionaler Klimamodellierung. Rep. Earth Syst. Sci. 125.
Goodwins, L., Menzies, B., Osborne, N., Muscatello, D., 2019. Human seasonal influenza and climate change: a systematic review of the methods used to examine the relationship between meteorological variables and influenza. Environ. Epidemiol. 3, 137. https://doi.org/10.1097/01.EE9.0000607256.48033.53, 2019 Annu. Conf. Int. Soc. Environ. Epidemiol. August 25–28 2019, Utrecht, Netherlands.
Grant, T., Croce, E., Matsui, E.C., 2022. Asthma and the social determinants of health. Ann. Allergy Asthma Immunol. 128, 5–11.
Guerrisi, C., Ecollan, M., Souty, C., Rossignol, L., Turbelin, C., Debin, M., Goronflot, T., Boëlle, P.-Y., Hanslik, T., Colizza, V., 2019. Factors associated with influenza-like-illness: a crowdsourced cohort study from 2012/13 to 2017/18. BMC Public Health 19, 1–9.
Hamaoui-Laguel, L., Vautard, R., Liu, L., Solmon, F., Viovy, N., Khvorostyanov, D., Essl, F., Chuine, I., Colette, A., Semenov, M.A., Schaffhauser, A., Storkey, J., Thibaudon, M., Epstein, M.M., 2015. Effects of climate change and seed dispersal on airborne ragweed pollen loads in Europe. Nat. Clim. Chang. https://doi.org/10.1038/nclimate2652.
Hao, L., Herrera-Avellanosa, D., Del Pero, C., Troi, A., 2020. What are the implications of climate change for retrofitted historic buildings? A literature review. Sustain. https://doi.org/10.3390/su12187557.
Hawkins, E., Frame, D., Harrington, L., Joshi, M., King, A., Rojas, M., Sutton, R., 2020. Observed emergence of the climate change signal: from the familiar to the unknown. Geophys. Res. Lett. https://doi.org/10.1029/2019GL086259.
Hirota, Y., Tekeshita, S., Ide, S., Kataoka, K., Ohkubo, A., Fukuyoshi, S., Takahashi, K., Hirohata, T., Kaji, M., 1992. Various factors associated with the manifestation of influenza-like illness. Int. J. Epidemiol. 21, 574–582.
Huijbregts, Z., Kramer, R.P., Martens, M.H.J., van Schijndel, A.W.M., Schellen, H.L., 2012. A proposed method to assess the damage risk of future climate change to museum objects in historic buildings. Build. Environ. https://doi.org/10.1016/j.buildenv.2012.01.008.
Hurraß, J., Heinzow, B., Aurbach, U., Bergmann, K.-C., Bufe, A., Buzina, W., Cornely, O.A., Engelhart, S., Fischer, G., Gabrio, T., Heinz, W., Herr, C.E.W., Kleine-Tebbe, J., Klimek, L., Köberle, M., Lichtnecker, H., Lob-Corzilius, T., Merget, R., Mülleneisen, N., Nowak, D., Rabe, U., Raulf, M., Seidl, H.P., Steiß, J.-O., Szewszyk, R., Thomas, P., Valtanen, K., Wiesmüller, G.A., 2017. Medical diagnostics for indoor mold exposure. Int. J. Hyg. Environ. Health 220, 305–328. https://doi.org/10.1016/j.ijheh.2016.11.012.
IPCC, 2013. Intergovernmental Panel on Climate Change Working Group I. Climate Change 2013: The Physical Science Basis. Long-term Climate Change: Projections, Commitments and Irreversibility. Cambridge Univ. Press, New York.
Jacob, D., Podzun, R., 1997. Sensitivity studies with the regional climate model REMO. Meteorog. Atmos. Phys. https://doi.org/10.1007/BF01025368.
Jacob, D., Haensler, A., Saeed, F., Elizalde, A., Hagemann, S., Kumar, P., Podzun, R., Rechid, D., Remedio, A.R., Sieck, K., Teichmann, C., Wilhelm, C., 2012. Assessing the transferability of the regional climate model REMO to different coordinated regional climate downscaling experiment (CORDEX) regions. Atmosphere (Basel). https://doi.org/10.3390/atmos3010181.
Jacob, D., Teichmann, C., Sobolowski, S., Katragkou, E., Anders, I., Belda, M., Benestad, R., Boberg, F., Buonomo, E., Cardoso, R.M., Casanueva, A., Christensen, O.B., Christensen, J.H., Coppola, E., De Cruz, L., Davin, E.L., Dobler, A., Domínguez, M., Fealy, R., Fernandez, J., Gaertner, M.A., García-Díez, M., Giorgi, F., Gobiet, A., Goergen, K., Gómez-Navarro, J.J., Alemán, J.J.G., Gutiérrez, C., Gutiérrez, J.M., Güttler, I., Haensler, A., Halenka, T., Jerez, S., Jiménez-Guerrero, P., Jones, R.G., Keuler, K., Kjellström, E., Knist, S., Kotlarski, S., Maraun, D., van Meijgaard, E., Mercogliano, P., Montávez, J.P., Navarra, A., Nikulin, G., de Noblet-Ducoudré, N., Panitz, H.J., Pfeifer, S., Piazza, M., Pichelli, E., Pietikäinen, J.P., Prein, A.F., Preuschmann, S., Rechid, D., Rockel, B., Romera, R., Sánchez, E., Sieck, K., Soares, P.

M.M., Somot, S., Srnec, L., Sørland, S.L., Termonia, P., Truhetz, H., Vautard, R., Warrach-Sagi, K., Wulfmeyer, V., 2020. Regional climate downscaling over Europe: perspectives from the EURO-CORDEX community. Reg. Environ. Chang. 20 https://doi.org/10.1007/s10113-020-01606-9.
Jain, S., Chaves, S.S., 2011. Obesity and influenza. Clin. Infect. Dis. 53 (5), 422–424.
Jin, L., Schubert, S., Fenner, D., Meier, F., Schneider, C., 2021. Integration of a building energy model in an urban climate model and its application. Boundary-Layer Meteorol. https://doi.org/10.1007/s10546-020-00569-y.
Johansson, P., Ekstrand-Tobin, A., Svensson, T., Bok, G., 2012. Laboratory study to determine the critical moisture level for mould growth on building materials. Int. Biodeterior. Biodegrad. https://doi.org/10.1016/j.ibiod.2012.05.014.
Kannabei, S., Dümmel, T., Hohlstein, G., Cobau-Lange, S., Basta, D., Bohnen, M., Kühsel, D., 2013. Berliner Aktionsprogramm gegen Ambrosia 2013. Berliner Aktionsprogr. gegen Ambrosia, FU-Berlin, p. 8.
Karki, S., Muscatello, D.J., Banks, E., MacIntyre, C.R., McIntyre, P., Liu, B., 2018. Association between body mass index and laboratory-confirmed influenza in middle aged and older adults: a prospective cohort study. Int. J. Obes. 42, 1480–1488.
Kay, D., Kelly, J., Schaeffer, T., Tuong, T., Leru, P., Addison, W.A., Neamtu, R., 2020. Pollen Allergies in Romania.
Kendon, E.J., Prein, A.F., Senior, C.A., Stirling, A., 2021. Challenges and outlook for convection-permitting climate modelling. Philos. Trans. R. Soc. A Math. Phys. Eng. Sci. https://doi.org/10.1098/rsta.2019.0547.
Kotlarski, S., Keuler, K., Christensen, O.B., Colette, A., Déqué, M., Gobiet, A., Goergen, K., Jacob, D., Lüthi, D., Van Meijgaard, E., Nikulin, G., Schär, C., Teichmann, C., Vautard, R., Warrach-Sagi, K., Wulfmeyer, V., 2014. Regional climate modeling on European scales: a joint standard evaluation of the EURO-CORDEX RCM ensemble. Geosci. Model Dev. 7, 1297–1333. https://doi.org/10.5194/gmd-7-1297-2014.
Kusunoki, T., Takeuchi, J., Morimoto, T., Sakuma, M., Yasumi, T., Nishikomori, R., Higashi, A., Heike, T., 2017. Fruit intake reduces the onset of respiratory allergic symptoms in schoolchildren. Pediatr. Allergy Immunol. 28, 793–800.
Laaidi, K., Laaidi, M., 1999. Airborne pollen of Ambrosia in Burgundy (France) 1996-1997. Aerobiologia (Bologna). https://doi.org/10.1023/A:1007547919559.
Langendijk, G.S., Rechid, D., Jacob, D., 2019. Urban areas and urban-rural contrasts under climate change: what does the EURO-CORDEX ensemble tell us?-investigating near surface humidity in berlin and its surroundings. Atmosphere (Basel). 10 https://doi.org/10.3390/ATMOS10120730.
Langendijk, G.S., Rechid, D., Sieck, K., Jacob, D., 2021. Added value of convection-permitting simulations for understanding future urban humidity extremes: case studies for Berlin and its surroundings. Weather Clim. Extrem. 33 https://doi.org/10.1016/j.wace.2021.100367.
Lauwaet, D., Hooyberghs, H., Lefebre, F., De Ridder, K., Willems, P., 2017. Climate-fit-City_D5.1: Urban Primary Data Need Analysis.
Leissner, J., Kilian, R., Kotova, L., Jacob, D., Mikolajewicz, U., Broström, T., Ashley-Smith, J., Schellen, H.L., Martens, M., Van Schijndel, J., Antretter, F., Winkler, M., Bertolin, C., Camuffo, D., Simeunovic, G., Vyhlídal, T., 2015. Climate for culture: assessing the impact of climate change on the future indoor climate in historic buildings using simulations. Herit. Sci. 3, 1–15. https://doi.org/10.1186/s40494-015-0067-9.
Leru, P.M., Kay, D., Kelly, J., Tuong, T., Schaeffer, T., Addison, B., Neamtu, R., 2021. Atopy and lifestyle survey of allergic patients from urban environment in Romania: preliminary data from an interactive qualifying project. Cureus 13.
Lin, L., Chan, T.O., Ge, E., Wang, X., Zhao, Y., Yang, Y., Ning, G., Zeng, Z., Luo, M., 2020. Effects of urban land expansion on decreasing atmospheric moisture in Guangdong, South China. Urban Clim. https://doi.org/10.1016/j.uclim.2020.100626.
Liu, L., Solmon, F., Vautard, R., Hamaoui-Laguel, L., Zsolt Torma, C., Giorgi, F., 2016. Ragweed pollen production and dispersion modelling within a regional climate system, calibration and application over Europe. Biogeosciences. https://doi.org/10.5194/bg-13-2769-2016.
Lokoshchenko, M.A., 2017. Urban heat island and urban dry island in Moscow and their centennial changes. J. Appl. Meteorol. Climatol. https://doi.org/10.1175/JAMC-D-16-0383.1.
Lourenço, P.B., Luso, E., Almeida, M.G., 2006. Defects and moisture problems in buildings from historical city centres: a case study in Portugal. Build. Environ. https://doi.org/10.1016/j.buildenv.2005.01.001.
Lowe, J.A., McSweeney, C., Hewitt, C., 2020. An Overview of the EUCP Project-towards Improved European Climate Predictions and Projections. EGU Gen. Assem. Conf. Abstr, p. 19475.
Lowen, A.C., Steel, J., 2014. Roles of humidity and temperature in shaping influenza seasonality. J. Virol. 88, 7692–7695. https://doi.org/10.1128/jvi.03544-13.
Lowen, A.C., Mubareka, S., Steel, J., Palese, P., 2007. Influenza virus transmission is dependent on relative humidity and temperature. PLoS Pathog. 3, 1470–1476. https://doi.org/10.1371/journal.ppat.0030151.
Majewski, D., 1991. The Europa-Modell of the Deutscher Wetterdienst. ECMWF Semin. Numer. methods Atmos. Model.
Marr, L.C., Tang, J.W., Van Mullekom, J., Lakdawala, S.S., 2019. Mechanistic insights into the effect of humidity on airborne influenza virus survival, transmission and incidence. J. R. Soc. Interface 16. https://doi.org/10.1098/rsif.2018.0298.
Masson, V., Lemonsu, A., Hidalgo, J., Voogt, J., 2020. Urban climates and climate change. Annu. Rev. Environ. Resour. 45, 411–444. https://doi.org/10.1146/annurev-environ-012320-083623.
Mendell, M.J., Kumagai, K., 2017. Observation-based metrics for residential dampness and mold with dose–response relationships to health: a review. Indoor Air 27, 506–517.
Meng, Y., Lu, Y., Xiang, H., Liu, S., 2021. Short-term effects of ambient air pollution on the incidence of influenza in Wuhan, China: a time-series analysis. Environ. Res. 192, 110327.
Menut, L., Vautard, R., Colette, A., Khvorostyanov, D., Potier, A., Hamaoui-Laguel, L., Viovy, N., Thibaudon, M., 2014. A new model of ragweed pollen release based on the analysis of meteorological conditions. Atmos. Chem. Phys. Discuss. https://doi.org/10.5194/acpd-14-10891-2014.
Moss, R.H., Edmonds, J.A., Hibbard, K.A., Manning, M.R., Rose, S.K., Van Vuuren, D.P., Carter, T.R., Emori, S., Kainuma, M., Kram, T., Meehl, G.A., Mitchell, J.F.B., Nakicenovic, N., Riahi, K., Smith, S.J., Stouffer, R.J., Thomson, A.M., Weyant, J.P., Wilbanks, T.J., 2010. The next generation of scenarios for climate change research and assessment. Nature. https://doi.org/10.1038/nature08823.
Murtas, R., Russo, A.G., 2019. Effects of pollution, low temperature and influenza syndrome on the excess mortality risk in winter 2016–2017. BMC Public Health 19, 1–9.
Nguyen, J.L., Schwartz, J., Dockery, D.W., 2014. The relationship between indoor and outdoor temperature, apparent temperature, relative humidity, and absolute humidity. Indoor Air. https://doi.org/10.1111/ina.12052.
Norbäck, D., 2020. Dampness, indoor mould and health. In: Indoor Environmental Quality and Health Risk toward Healthier Environment for all. Springer, pp. 199–216.
Noti, J.D., Blachere, F.M., McMillen, C.M., Lindsley, W.G., Kashon, M.L., Slaughter, D.R., Beezhold, D.H., 2013. High humidity leads to loss of infectious influenza virus from simulated coughs. PLoS One 8, 2–9. https://doi.org/10.1371/journal.pone.0057485.
Ojanen, T., Viitanen, Hannu, Lähdesmäki, K., Vinha, J., Peuhkuri, R., Salminen, K., 2010. Mold Growth Modeling of Building Structures Using Sensitivity Classes of Materials Tuomo. Acta Acust. united with Acust.
Park, J.E., Son, W.S., Ryu, Y., Choi, S.B., Kwon, O., Ahn, I., 2020. Effects of temperature, humidity, and diurnal temperature range on influenza incidence in a temperate region. Influenza Other Respir. Viruses 14, 11–18. https://doi.org/10.1111/irv.12682.
Peci, A., Winter, A.L., Li, Y., Gnaneshan, S., Liu, J., Mubareka, S., Gubbay, J.B., 2019. Effects of absolute humidity, relative humidity, temperature, and wind speed on influenza activity in Toronto, Ontario, Canada. Appl. Environ. Microbiol. 85, 1–13. https://doi.org/10.1128/AEM.02426-18.
Pflanzenschutzamt Berlin, 2021, https://www.berlin.de/pflanzenschutzamt/stadtgruen/ambrosia-bekaempfung/, (accessed: 21.05.2021).
Pietrzyk, K., 2015. A systemic approach to moisture problems in buildings for mould safety modelling. Build. Environ. https://doi.org/10.1016/j.buildenv.2014.12.013.
Prank, M., Chapman, D.S., Bullock, J.M., Belmonte, J., Berger, U., Dahl, A., Jäger, S., Kovtunenko, I., Magyar, D., Niemelä, S., Rantio-Lehtimäki, A., Rodinkova, V., Sauliene, I., Severova, E., Sikoparija, B., Sofiev, M., 2013. An operational model for forecasting ragweed pollen release and dispersion in Europe. Agric. For. Meteorol. 182–183, 43–53. https://doi.org/10.1016/J.AGRFORMET.2013.08.003.

Prein, A.F., Langhans, W., Fosser, G., Ferrone, A., Ban, N., Goergen, K., Keller, M., Tölle, M., Gutjahr, O., Feser, F., Brisson, E., Kollet, S., Schmidli, J., Van Lipzig, N.P. M., Leung, R., 2015. A review on regional convection-permitting climate modeling: demonstrations, prospects, and challenges. Rev. Geophys. 53, 323–361. https://doi.org/10.1002/2014RG000475.

Rechid, D., Jacob, D., 2006. Influence of monthly varying vegetation on the simulated climate in Europe. Meteorol. Z. 15, 99–116. https://doi.org/10.1127/0941-2948/2006/0091.

Reinhardt, F., Herle, M., Bastiansen, F., Streit, B., 2003. Ökonomische Folgen der Ausbreitung von Neobiota, pp. 1–248.

Ritschkoff, A.C., Viitanen, H., Koskela, K., 2000. The response of building materials to the mould exposure at different humidity and temperature conditions. In: Healthy Buildings 2000, pp. 317–322.

RKI, 2019. Pommes für die Grippeschutzimpfung? Neuer Influenza-Saisonbericht erschienenPommes für die Grippeschutzimpfung? Neuer Influenza-Saisonbericht erschienen [WWW Document]. URL. https://www.rki.de/DE/Content/Service/Presse/Pressemitteilungen/2019/10_2019.html (accessed 2.18.21).

RKI, 2020. Brandenburg und Berlin - Saison 2020/2021, Arbeitsgemeinschaft Influenza [WWW Document]. URL. https://influenza.rki.de/Diagrams.aspx?agiRegion=3 (accessed 2.18.21).

Roeckner, E., Arpe, K., Bengtsson, L., Christoph, M., Claussen, M., Dümenil, L., Esch, M., Giorgetta, M., Schlese, U., Schulzweida, U., 1996. The atmospheric general circulation model ECHAM-4: model description and simulation of present-day climate. MPI Rep. 218, 171.

Rosenzweig, C., Solecki, W., Romero-Lankao, P., Mehrotra, S., Dhakal, S., Bowman, T., Ibrahim, S.A., 2018. Climate Change and Cities: Second Assessment Report of the Urban Climate Change Research Network, in: Climate Change and Cities. https://doi.org/10.1017/9781316563878.007.

Sedghy, F., Varasteh, A.-R., Sankian, M., Moghadam, M., 2018. Interaction between air pollutants and pollen grains: the role on the rising trend in allergy. Reports Biochem. Mol. Biol. 6, 219.

Sedlbauer, K., 2001. Prediction of Mould Fungus Formation on the Surface of/and inside Building Components.

Seguel, J.M., Merrill, R., Seguel, D., Campagna, A.C., 2017. Indoor air quality. Am. J. Lifestyle Med. 11, 284–295.

Semmler, T., 2002. Der Wasser- und Energiehaushalt der arktischen Atmosphäre. Examensarbeit - Max-Planck-Institut fur Meteorol. 101–106.

Shaman, J., Kohn, M., 2009. Absolute humidity modulates influenza survival, transmission, and seasonality. Proc. Natl. Acad. Sci. 106, 3243–3248. https://doi.org/10.1073/PNAS.0806852106.

Shaman, J., Pitzer, V.E., Viboud, C., Grenfell, B.T., Lipsitch, M., 2010. Absolute humidity and the seasonal onset of influenza in the continental United States. PLoS Biol. 8 https://doi.org/10.1371/journal.pbio.1000316.

Shaman, J., Goldstein, E., Lipsitch, M., 2011. Absolute humidity and pandemic versus epidemic influenza. Am. J. Epidemiol. 173, 127–135. https://doi.org/10.1093/aje/kwq347.

Silverberg, J.I., Braunstein, M., Lee-Wong, M., 2015. Association between climate factors, pollen counts, and childhood hay fever prevalence in the United States. J. Allergy Clin. Immunol. https://doi.org/10.1016/j.jaci.2014.08.003.

Sinclair, R., Russell, C., Kray, G., Vesper, S., 2018. Asthma risk associated with indoor mold contamination in hispanic communities in Eastern Coachella Valley, California. J. Environ. Public Health 2018.

Soebiyanto, R.P., Gross, D., Jorgensen, P., Buda, S., Bromberg, M., Kaufman, Z., Prosenc, K., Socan, M., Alonso, T.V., Widdowson, M.A., Kiang, R.K., Shaman, J., 2015. Associations between meteorological parameters and influenza activity in Berlin (Germany), Ljubljana (Slovenia), Castile and León (Spain) and Israeli districts. PLoS One 10, 1–21. https://doi.org/10.1371/journal.pone.0134701.

Sofiev, M., Siljamo, P., Ranta, H., Linkosalo, T., Jaeger, S., Rasmussen, A., Rantio-Lehtimaki, A., Severova, E., Kukkonen, J., 2013. A numerical model of birch pollen emission and dispersion in the atmosphere. Description of the emission module. Int. J. Biometeorol. 57, 45–58. https://doi.org/10.1007/s00484-012-0532-z.

Song, Y., Zhang, Y., Wang, T., Qian, S., Wang, S., 2021. Spatio-temporal differentiation in the incidence of influenza and its relationship with air pollution in China from 2004 to 2017. Chin. Geogr. Sci. 31, 815–828.

SSW, 2018. Senatsverwaltung für Stadtentwicklung und Wohnen: Gebäudealter der Wohnbebauung (Ausgabe 2018).

Stevens, B., Giorgetta, M., Esch, M., Mauritsen, T., Crueger, T., Rast, S., Salzmann, M., Schmidt, H., Bader, J., Block, K., Brokopf, R., Fast, I., Kinne, S., Kornblueh, L., Lohmann, U., Pincus, R., Reichler, T., Roeckner, E., 2013. Atmospheric component of the MPI-M earth system model: ECHAM6. J. Adv. Model. Earth Syst. 5, 146–172. https://doi.org/10.1002/jame.20015.

Storkey, J., Stratonovitch, P., Chapman, D.S., Vidotto, F., Semenov, M.A., 2014. A process-based approach to predicting the effect of climate change on the distribution of an invasive allergenic plant in Europe. PLoS One 9. https://doi.org/10.1371/journal.pone.0088156.

Stull, R., 2017. Practical Meteorology: An Algebra-Based Survey of Atmospheric Science. Univ. of British Columbia.

Su, W., Wu, X., Geng, X., Zhao, X., Liu, Q., Liu, T., 2019. The short-term effects of air pollutants on influenza-like illness in Jinan, China. BMC Public Health 19, 1–12.

Toczylowski, K., Wietlicka-Piszcz, M., Grabowska, M., Sulik, A., 2021. Cumulative effects of particulate matter pollution and meteorological variables on the risk of influenza-like illness. Viruses 13, 556.

Towers, S., Chowell, G., Hameed, R., Jastrebski, M., Khan, M., Meeks, J., Mubayi, A., Harris, G., 2013. Climate change and influenza: the likelihood of early and severe influenza seasons following warmer than average winters. PLoS currents 5.

Trusilova, K., Früh, B., Brienen, S., Walter, A., Masson, V., Pigeon, G., Becker, P., 2013. Implementation of an urban parameterization scheme into the regional climate model COSMO-CLM. J. Appl. Meteorol. Climatol. 52 (10), 2296–2311. https://doi.org/10.1175/JAMC-D-12-0209.1.

Viitanen, H., Ojanen, T., 2007. Improved model to predict mold growth in building materials. Thermal Performance of the Exterior Envelopes of Whole Buildings X–Proceedings CD 2–7.

Viitanen, H., Toratti, T., Makkonen, L., Peuhkuri, R., Ojanen, T., Ruokolainen, L., Räisänen, J., 2010. Towards modelling of decay risk of wooden materials. Eur. J. Wood Wood Prod. https://doi.org/10.1007/s00107-010-0450-x.

Voros, K., Bobvos, J., Varró, J.M., Mainasi, T., Rudnai, P., Paldy, A., 2018. Impacts of long-term ragweed pollen load and other potential risk factors on ragweed pollen allergy among schoolchildren in Hungary. Ann. Agric. Environ. Med. 25.

Wang, B., Liu, Y., Li, Zhenjiang, Li, Zhiwen, 2016. Association of indoor air pollution from coal combustion with influenza-like illness in housewives. Environ. Pollut. 216, 646–652.

WHO, W.H.O, 2010. Sex, gender and influenza. World Health Organisation, Geneva.

Wiesmüller, G.A., Heinzow, B., Aurbach, U., Bergmann, K.-C., Bufe, A., Buzina, W., Cornely, O.A., Engelhart, S., Fischer, G., Gabrio, T., 2016. AWMF-Schimmelpilz-Leitlinie "Medizinisch klinische Diagnostik bei Schimmelpilzexposition in Innenräumen" AWMF-Register-Nr. 161/001-Endfassung.

Wong, C.M., Yang, L., Chan, K.P., Chan, W.M., Song, L., Lai, H.K., Thach, T.Q., Ho, L.M., Chan, K.H., Lam, T.H., 2013. Cigarette smoking as a risk factor for influenza-associated mortality: evidence from an elderly cohort. Influenza Other Respir. Viruses 7, 531–539.

Yang, L., Chan, K.P., Lee, R.S., Chan, W.M., Lai, H.K., Thach, T.Q., Chan, K.H., Lam, T.H., Peiris, J.S.M., Wong, C.M., 2013. Obesity and influenza associated mortality: evidence from an elderly cohort in Hong Kong. Prev. Med. (Baltim). 56, 118–123.

Zhao, L., Oleson, K., Bou-Zeid, E., Krayenhoff, E.S., Bray, A., Zhu, Q., Zheng, Z., Chen, C., Oppenheimer, M., 2021. Global multi-model projections of local urban climates. Nat. Clim. Chang. https://doi.org/10.1038/s41558-020-00958-8.

Zink, K., Vogel, H., Vogel, B., Magyar, D., Kottmeier, C., 2012. Modeling the dispersion of Ambrosia artemisiifolia L. pollen with the model system COSMO-ART. Int. J. Biometeorol. 669–680.

Ziska, L.H., Gebhard, D.E., Frenz, D.A., Faulkner, S., Singer, B.D., Straka, J.G., 2003. Cities as harbingers of climate change: common ragweed, urbanization, and public health. J. Allergy Clin. Immunol. 111, 290–295. https://doi.org/10.1067/mai.2003.53.